

UCID--19976

DE84 005221

MINERALOGIC AND PETROLOGIC INVESTIGATION
OF PRE-TEST CORE SAMPLES
FROM THE SPENT FUEL TEST-CLIMAX

F. J. FRERSON
B. J. QUALHEIM

DECEMBER 1983

The logo for Lawrence Livermore Laboratory is a large, stylized, downward-pointing chevron shape. The top horizontal edge of the chevron is filled with a fine, stippled texture. The two slanted sides of the chevron are filled with a solid black color. The text "Lawrence Livermore Laboratory" is printed in a bold, sans-serif font, oriented diagonally to follow the right-hand slanted edge of the chevron. A small, solid black arrowhead points downwards from the top edge of the chevron towards the text.

Lawrence
Livermore
Laboratory

This is an informal report intended primarily for internal or limited external distribution. The opinions and conclusions stated are those of the author and may or may not be those of the Laboratory.

Work performed under the auspices of the U.S. Department of Energy by the Lawrence Livermore Laboratory under Contract W-7405-Eng-43.

Mineralogic and Petrologic Investigation
of Pre-Test Core Samples
from the Spent Fuel Test-Climax

by

F.J. Ryerson and E.J. Qualheim

DISCLAIMER

This report was prepared as an account of work sponsored by an agency of the United States Government. Neither the United States Government nor any agency thereof, nor any of their employees, makes any warranty, express or implied, or assumes any legal liability or responsibility for the accuracy, completeness, or usefulness of any information, apparatus, product, or process disclosed, or represents that its use would not infringe privately owned rights. Reference herein to any specific commercial product, process, or service by trade name, trademark, manufacturer, or otherwise does not necessarily constitute or imply its endorsement, recommendation, or favoring by the United States Government or any agency thereof. The views and opinions of authors expressed herein do not necessarily state or reflect those of the United States Government or any agency thereof.

DISTRIBUTION OF THIS DOCUMENT IS UNLIMITED

EJB

ABSTRACT

Pre-test samples obtained from just inside the perimeter of the canister emplacement holes at the Spent Fuel Test-Climax have been characterized by petrographic and microanalytical techniques. The primary quartz monzonite has undergone various degrees of hydrothermal alteration as a result of natural processes. Alteration is most apparent on primary plagioclase and biotite. The most common secondary phases on plagioclase are muscovite and calcite, while the most common secondary phases on biotite are epidote and chlorite. The major alteration zones encountered are localized along filled fractures, i.e. veins. The thickness and mineralogy of the alteration zones can be correlated with the vein mineralogy, becoming wider and more complex mineralogically when the veins contain calcite.

INTRODUCTION

The Spent Fuel Test-Climax (SFT-C) is being conducted under the technical direction of the Lawrence Livermore National Laboratory as part of the U.S. Department of Energy's Nevada Nuclear Waste Storage Investigations (NNWSI). The main objective of the SFT-C is to evaluate the technical feasibility of short-term emplacement and retrieval of spent reactor fuel assemblies at plausible repository depth in granitic rocks (Ramspott et al., 1979). A secondary, though equally important, objective is the evaluation of a typical granitic rock's response to the thermal and radiation fields produced by the spent fuel assemblies. Simply, how are the physical, thermal and mineralogical properties of the country rock altered during the course of exposure? These data are necessary if granitic rocks are to be qualified as possible long-term repositories for either spent fuel or reprocessed commercial and military reactor waste.

In this report we present mineralogical and petrological data from the characterization of samples from the 17 canister core holes (CCH 1-17). These cores were obtained from just inside the perimeter of emplacement holes which were subsequently hammer drilled to 0.61 m. diameter and loaded with either spent fuel assemblies (1, 3, 5, 7-12, 14, 16) or electrical simulators (2, 4, 6, 13, 15, 17) (Ramspott et al., 1981). The purpose of this investigation is to provide a data base of mineralogical compositions, assemblages and modal proportions from pre-test samples to serve as a comparison to a similar data base that will be obtained from post-test samples. The post-test core samples will be obtained from just outside the perimeter of the canister emplacement holes directly adjacent (along a radius) to the pre-test core. This should allow us to determine whether or not any mineralogical changes have occurred during the course of the test. The close proximity of the pre- and post-test cores should also enable us to assess the possible migration of spent fuel, canister and/or alteration generated material along the various types of fractures in the quartz monzonite. The effects of spent fuel assemblies versus electrical simulators may also be investigated. In a more general application, detailed petrologic and mineralogic data is a necessity if the results of mechanical and thermal tests of these samples are to be fully understood.

In formulating an approach to this task it is worthwhile to consider the types of mineralogical phenomena that could occur during the time the fuel assemblies and electrical simulators are in place. Those that can alter mineralogic properties are:

- 1) hydration reactions
- 2) dehydration reactions
- 3) precipitation of new phases from solution
- 4) cation exchange

The first two processes can be evaluated, in large part, with strictly petrographic observations of mineral assemblages regarding the presence or absence of key mineral phases. This is also true of the third process, although the possibility that a primary mineral may dissolve and then reprecipitate as a mineral of the same solid-solution series with a different composition cannot be overlooked.

The observation of the third process requires compositional data and, clearly, so do changes caused by the fourth process, cation exchange. As such, our approach is one of combined petrographic analysis and compositional analysis by electron microprobe techniques.

GEOLOGIC SETTING

The Climax stock, located on the U.S. Department of Energy's Nevada Test Site (NTS), is a composite granitic pluton composed of an equigranular biotite granodiorite and a porphyritic biotite quartz monzonite. The Cretaceous Age pluton is intruded into Paleozoic carbonate rocks (Maldonado, 1977). The intrusion has caused recrystallization of the carbonates to form marbles, and locally tungsten-bearing skarns are present. The SFT-C tunnel complex lies entirely within the quartz monzonite.

PREVIOUS INVESTIGATIONS

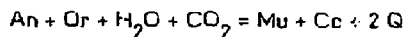
Connolly (1981) has studied the hydrothermal alteration of rocks from the SFT-C tunnel complex. This work provides an excellent background for the present study as it is not restricted to wall-rock alteration in samples from only the CCH's, where the alteration is structurally controlled and often poorly developed. His work concentrates upon alteration zones approximately 5m^3 in extent which display no apparent control by structural features. The larger spatial extent of the unlocalized alteration assemblages allows more meaningful modal characterization of the alteration assemblages (Table 1).

Including the pervasive deuteric alteration, five alteration types are observed: deuteric, propylitic, argillic, phyllic, and potassic (Connolly, 1981). These alteration zones are often sharply defined and concentrically arranged progressing inward from deuteric to potassic. The average modes indicate that the presence or absence of certain key phases in the these alteration zones may be useful in classifying the structurally controlled localized wall-rock alteration zones (Table 1). The potassic alteration is characterized by the high modal abundance of K-feldspar (57 vol.%) and low modal

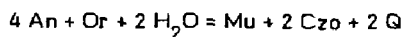
abundance of quartz (5 vol.%). Phyllic alteration is characterized by high modal abundances of muscovite (30%) and calcite (5 vol.%). The presence of kaolinite distinguishes argillic alteration; kaolinite has not been observed in any of the CCH samples characterized in this study. Deuteric and propylitic assemblages have quite similar modal abundances for almost all phases. Rutile, hematite and kaolinite are present in the propylitic assemblage, but not in the deuteric; however, their abundances are insignificant. This modal similarity, coupled with the relatively poor development (i.e., limited spatial extent and overprinting) of the localized alteration, make it impossible to distinguish deuteric from propylitic alteration zones in localized alteration. Hence, both possibilities will be designated as deuteric alteration.

The assemblages observed in the localized wall-rock alteration record either multiple alteration events or a single event with continuously variable temperature and fluid conditions. As such, the determination of physical conditions during alteration is equivocal. The better developed unlocalized wall-rock assemblages allow more reliable determination of these conditions. This data is important as it allows the possible range of physical conditions encountered subsequent to spent fuel and electrica simulator storage to be compared with the conditions encountered during hydrothermal alteration.

Connolly (1981) has estimated the external conditions for both deuteric and potassic alteration. In the deuteric zone, the thermodynamic expressions for the reactions



and



can be solved simultaneously along with the condition that the fluid is a binary $\text{CO}_2\text{-H}_2\text{O}$ phase to yield a temperature of 370°C, $X(\text{CO}_2)=0.018$. The ambient pressure determined by reconstruction of overburden is approximately 1 Kb (Ketner 1956, 1957; Barnes et al., 1963).

The temperatures within the potassic zone are estimated from the two-feldspar geothermometer (Whitney and Stormer, 1977) and range between 335-430°C. The maximum temperature experienced by the rock near the spent fuel canisters is 85°C (Patrick et al. 1981), hence, the conditions encountered during hydrothermal alteration were far in excess of those during the SFT-C.

METHODS OF STUDY

Sample Selection

All samples described in this study were taken from cores obtained from inside the perimeter of the 17 canister emplacement holes. A reference line was drawn longitudinally along the recovered core. This reference line was then used to measure distances along the core and to determine the relative orientations of fractures for logging and sample selection.

The location and orientation of all fractures and alteration zones in the 17 core samples was recorded at NTS. Using these core logs, 1- to 2-foot sections of core were selected using the following criteria:

- 1) top of core
- 2) bottom of core
- 3) sample representing (as closely as possible) "fresh" unaltered rock free of fractures, i.e., "bulk sample"
- 4) samples encompassing all the different types of alteration that could be described in hand specimen (it turns out that much of the sampling was redundant)

Criteria 1-3 were fulfilled for each hole. Criterion 4 was only applied to holes of specific interest. The 1- to 2-foot core sections were then returned to LLNL for further selection.

After selecting the desired sample areas, a disk of the section cut perpendicular to the reference line was removed from the core. This disk was then cut in half (parallel to the reference line) and one piece retained at LLNL while the other was sent offsite for the preparation of polished thin sections.

Petrography and Modal Analysis

All thin sections were observed in plane and cross-polarized transmitted light in order to determine mineral assemblages and textures (Appendix A). A number of samples were then point counted (2000 point modes) in transmitted light in order to determine modal abundances. The samples selected for modal analyses are:

- 1) all samples from CCH-1
- 2) the "bulk sample" from each hole

Samples from group (1) are used to demonstrate the variation in modal abundances in a specific hole. These variations are due to alteration and vein injection. The group (2) samples were chosen as "fresh" rock. Modal variations among these samples should, therefore, demonstrate the range of modal abundances in unaltered rock as a function of position along the canister drift.

Microprobe Analysis

Microprobe analyses were obtained in both automated and interactive modes employing a $2\mu\text{m} \times 2\mu\text{m}$ rastered beam at 15 na sample current (measured in a Faraday cup) with an accelerating voltage of 15 kV. The totally automated analyses were undertaken in order to objectively determine the frequency of K-feldspar and plagioclase compositions within selected samples. In this mode 300 analyses were obtained along a grid covering the sample surface. Approximately 600 12-element analyses were obtained in a 24-hour period. The interactive analysis required operator selection of specific analysis points. This was done in order to determine the compositions of alteration phases which are normally low in the mode.

PETROGRAPHY

Unaltered Rock

The quartz monzonite is a porphyritic rock composed of a groundmass which is predominately equant, subhedral grains of plagioclase, K-feldspar, quartz, and biotite ranging in size from 0.5-2.0 mm in diameter. Igneous accessory phases (titanite, allanite, zircon, and apatite) are below 3 volume % and show no effects of hydrothermal alteration (Conrally, 1981).

Plagioclase in the groundmass is tabular and elongate. Oscillatory zoning is a common feature, and polysynthetic twinning is ubiquitous. Plagioclase commonly contains inclusions of clinozoisite, epidote and calcite associated with hydrothermal alteration.

Quartz and K-feldspar are present both in the groundmass and as phenocrysts. In the groundmass both have anhedral to subhedral granular habits. The K-feldspars are untwinned, and the quartz commonly displays undulatory extinction. Phenocrysts of K-feldspar (4-6 mm in length) are anhedral and commonly perthitic. Quartz phenocrysts (3-15 mm) are commonly composed of a number of smaller grains.

Biotite has a tabular habit and can be as large as 1 mm. Biotite is commonly altered to some subset of the minerals chlorite, muscovite, epidote, titanite, rutile, calcite, and pyrite.

Vein Mineralogy

Two distinctly different types of mineral assemblages are found in the veins within the canister drift region. The first vein, henceforth referred to as "barren," is composed of quartz with or without pyrite. Alteration zones adjacent to the barren veins are typically thin (<5 mm) and lack intense secondary mineralization. In particular, calcite is never found in these alteration zones.

The second vein assemblage is composed of quartz, calcite, pyrite, and apatite. It may also contain grains of muscovite, K-feldspar and intensely altered plagioclase. The alteration zones adjacent to these "fertile" veins can be as large as 2 cm in diameter and often show intense alteration.

Alteration of Plagioclase

Plagioclase from the Climax stock is almost always altered to some combination of muscovite, epidote and calcite (Table II). The alteration assemblages found here are similar to those described by Ferry (1979) for mesozonal granitic plutons. The most common assemblages are (a) plagioclase and muscovite and (b) plagioclase, muscovite and calcite which are found in 43% and 35% of the sample areas studied, respectively (Appendix A). *The alteration phases generally have irregular outlines, although muscovite is often present as fan-shaped aggregates.* The percentage of plagioclase converted in a single grain can range from 0-75 volume %, and the distribution of converted and unconverted is sporadic although greater conversion is noted near veins.

Photomicrographs of typical plagioclase alteration assemblages are presented in Figure 1. It should also be noted that the plagioclase alteration assemblages can be correlated with the vein mineral assemblage about which they are localized. Assemblages B and D (from Table II) are usually found adjacent to "barren" veins, while assemblages C and E are found adjacent to "fertile" veins.

In characterizing the plagioclase alteration assemblages, we have chosen not to distinguish clinozoisite from iron-bearing epidote. The complex zoning patterns make such a separation quite cumbersome for these samples. Figure 2 shows a backscattered electron image and corresponding Fe_K X-ray image of an "epidote" grain included in altered plagioclase. The image illustrates discontinuous oscillatory zoning on a 10 μm scale in which the grain has compositions ranging from pure clinozoisite to Fe-rich epidote.

Alteration of Biotite

The alteration of biotite in these samples is extremely complex and makes any classification scheme quite difficult. The secondary phases found on biotite include chlorite, muscovite, epidote, titanite, rutile, calcite, and pyrite (Appendix A). In any particular sample, the number of phases found on biotite may vary. For instance, one biotite grain may include only chlorite while an adjacent grain contains chlorite and epidote. We have chosen to base our classification scheme on the maximum number of phases found on biotite rather than on the most frequent assemblage. The variability and, in some cases, large number of phases may be related to variability in the pore fluid composition during alteration and/or the variability in cation transport paths within the rocks.

A large variety of alteration assemblages are found on biotite (Table III). The most common assemblages are (a) biotite and chlorite, and (b) biotite, chlorite and epidote and (c) chlorite, muscovite, epidote, and titanite which are found in 23%, 20% and 13%, respectively, of the samples classified.

The alteration assemblages in Table III record a progressive loss of iron and magnesium from the biotite sites. This is first seen by the replacement of biotite by chlorite. Chlorite appears as symplectic intergrowths in biotite (Fig. 3a). A similar texture is observed in biotite-chlorite-epidote assemblages where biotite intergrowths are often crosscut by anhedral euhedral grains of epidote (Fig. 3b and c). Further depletion of iron and magnesium results in the complete disappearance of biotite. This often results in symplectic intergrowths of muscovite and chlorite which include scattered anhedral grains of epidote or titanite and/or rutile needles (Fig. 3d-f). Eventually, even chlorite may disappear leaving assemblages that are predominantly muscovite. An additional feature of the biotite-free samples is the presence of calcite after biotite. The calcite commonly appears along cleavage traces in chlorite or muscovite but may also be found as anhedral grains with these phases (Fig. 3j).

Modal Analyses

Results of modal analyses for CCH-1 samples and "bulk samples" from each of the 17 CCH's are presented in volume % and were obtained from 2000 point modes (Appendix B). Percentages of key phases have been plotted against sample position in Figures 4 and 5.

Modal analyses for the CCH-1 were obtained from the entire thin section regardless of any sample heterogeneity. Material from veins, alteration zones and unaltered regions were all counted equally in order that sample variability on this scale could be documented. Modal percentages for the primary phases, quartz, plagioclase, and K-feldspar, are fairly constant with average modal volumes of $17.3\% \pm 2.1\%$, $32.8\% \pm 5.6\%$ and $31.2\% \pm 5.3\%$, respectively. The 1-sigma variation for plagioclase and K-feldspar are similar in spite of the much more pronounced alteration of plagioclase. Biotite is also a primary phase but displays a much larger percent variation than do the felsic phases. The average biotite volume is $4.9 \pm 2.7\%$. The higher variability in biotite abundance is consistent with textural variability demonstrated earlier for biotite alteration.

Muscovite, chlorite, epidote, clinozoisite, titanite, and pyrite are present as secondary minerals. Their secondary origin is reflected in much larger variations in their modal abundance (Table IV, Fig. 4) and results from both variability in alteration down CCH-1 and to the presence or absence of veins which carried the hydrothermal solutions.

The modal abundances for the "bulk samples" have not been collected in a manner which includes the larger phenocrysts, and therefore, cannot be compared directly with the data in Table I in which only the groundmass phases were counted (the high modal abundance of K-feldspar phenocrysts may account for the generally lower abundance of quartz and higher modal abundance of K-feldspar in our data as compared to that of Connolly (1981)). Of the primary phases, only plagioclase appears to be significantly higher in the fresh "bulk samples" than in the variably altered samples from CCH-1, 42.8% versus 32.8%, respectively. This is consistent with the observation that plagioclase is the only felsic phase which undergoes significant alteration.

The modal volumes of the secondary phases are as variable in the "bulk samples" as in those from CCH-1 (Table V, Fig. 5). However, the average volumes of secondary phases in the bulk samples has decreased.

MINERAL CHEMISTRY

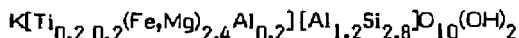
Primary Phases

The major primary igneous phases are quartz, plagioclase, K-feldspar, and biotite. Analyses obtained in the interactive mode are presented in Appendix C. In addition to interactive analyses, feldspar analyses were also obtained by automated step-scan traverses in order to objectively determine the extent of zoning and average feldspar compositions (Fig. 6).

Histograms of feldspar analyses obtained from step-scan traverses indicate that the K-feldspar analyses vary between Or_{80} and Or_{98} with only occasional analyses falling at lower Or concentrations. The average analysis is Or_{90} , and shows very little variation from sample to sample. These values agree quite well with those obtained during the interactive analyses (Fig. 7). The K-feldspars show very little alteration, so that the variation must be due to a combination of primary igneous zoning coupled with subsolidus reequilibration.

The majority of the plagioclase composition fall between An_{20} - An_{50} with the average at An_{33} (Fig. 6). Again, sample-to-sample variation in average analysis and frequency is small. In contrast to the K-feldspar analyses, comparison of the plagioclase analyses collected in automated and interactive analyses show an important difference (Figs. 6 and 7). The interactive analyses focused upon plagioclase grains which contained significant amounts of secondary phases. This group of analyses contains significantly more analyses in the range An_{20} - An_0 than do those obtained in the automated step-scan traverses. This feature, which has also been observed by Ferry (1979), is indicative of incongruent plagioclase alteration. The albite endmember is conserved during hydrothermal alteration, while the anorthite component is preferentially dissolved and transported from the plagioclase site.

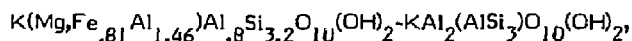
The biotite analyses can be represented by the formula,



The Mg/(Mg+Fe) ratio in these biotites lies between 0.50 and 0.68 (Fig. 8).

Secondary Phases

All data for secondary minerals was collected in an interactive mode and is presented in Appendix C. The muscovite compositions fall in the range approximated by the formula,



with a range in Mg/(Mg+Fe) (atom) between 0 and 1.0. When projected onto the plane $(Al_2O_3 - K_2O) - MgO - FeO$ from quartz, K-feldspar and H_2O , it can be shown that the muscovites which are found to be pseudomorphing biotites are generally enriched in MgO and FeO relative to those found on plagioclase (Fig. 9). This is most likely indicative of increased activities of the components on the biotite sites and indicates that cation exchange equilibrium between plagioclase and biotite sites was not attained on even a thin section scale during hydrothermal alteration.

Chlorite is found exclusively on biotite sites, and its composition is given by the formula $(Fe, Mg)_{4.4} Mn_{.1} Al_{2.6} Si_{2.7} O_{10} (OH)_2$. The range in Mg/(Mg+Fe) is between 0.42 and 0.74 and is slightly larger than the range for the primary biotite (Fig. 8).

Mineral compositions and zoning patterns in the clinzoisite-epidote series are complex. The compositions are generally expressed by the formula $Ca_2 (Al, Fe^{3+})_3 Si_3 O_{12} (OH)$. Given the complexity of the zonation, we have arbitrarily tabulated the analyses of this phase on plagioclase as "clinzoisite" and those on biotite as "epidote" (Appendix C). Generally, the "epidotes" found on biotite are more iron-rich than the "clinzoisites" found on plagioclase. The Al/(Al+Fe) in the epidotes ranges from 0.86-0.68 while that in the clinzoisites varies between 0.99 and 0.79. A large variation in Al/(Al+Fe) can occur in a single grain of clinzoisite. For instance, the analyses of clinzoisites found on a single grain of "clinzoisite" in plagioclase (Fig. 2) cover a large portion of the field of clinzoisite-epidote analyses encountered in the entire study area (Fig. 10).

For all practical purposes, the composition of pyrite can be assumed as FeS_2 and titanite as CaTiSiO_5 . The calcite composition is given by the formula $\text{Ca}_{.98}\text{Mg}_{.01}\text{Fe}_{.01}\text{CO}_3$.

SUMMARY

The data presented in this report document the chemical, petrographic and modal variations in core samples from the canister drift from the SFT-C. On a thin section scale (3 x 5 mm.) significant variations in all of these properties are found. The variations result from both igneous processes and hydrothermal alteration localized along fractures.

Variations due to primary igneous processes include zonation in plagioclase and K-feldspar within a particular section. The range and frequency of feldspar compositions has been documented through the use of an automated step-scanning procedure on an electron microprobe. Modal variations exist primarily due to the presence or absence of quartz and K-feldspar phenocrysts. It is worthwhile to note that chemical analyses of 500 cm^3 samples displayed relatively smaller sample-to-sample variations than did modal analyses of thin sections 15 cm^2 (Connolly, 1981). This is due to the relatively smaller contribution of phenocryst variations in the larger samples and should be considered in designing tests of physical properties for these rocks.

Features due to hydrothermal alteration are highly variable both within a particular section as well as between samples. Alteration zones (up to 2 cm wide) are localized along veins. The actual assemblages of secondary phases can be quite variable from sample to sample and from grain to grain of primary mineral phase. The compositions of some secondary phases (muscovite and epidote) can be shown to vary between different primary phase reaction sites, documenting gradients in chemical potentials of these components during hydrothermal alteration. The alteration assemblages also demonstrate that CO_2 , S and H_2O were added to the rock during hydrothermal alteration. The source of this material is presumably the decarbonation of the carbonate country rock during the emplacement of the stock.

REFERENCES

- Connolly, J.A., "Hydrothermal alteration in the Climax granite stock at the Nevada Test Site," Arizona State University, Tempe, AZ., unpublished M.S. Thesis. (1981)
- Ferry, J.M., "Reaction mechanisms, physical conditions and mass transfer during hydrothermal alteration of mica and feldspar in granitic rocks from south-central Maine, U.S.A.," *Contrib. Mineral. Petrol.*, **68**, 125-139, (1979)
- Maldonado, F., "Summary of geology and physical properties of the Climax Stock Nevada Test Site," Open File Report 77-356, U.S. Geological Survey, Washington, D.C. (1977)
- Patrick, W.C., L.B. Ballou, T.R. Butkovitch, R.C. Carlson, W.B. Durham, G.L. Hage, E.L. Majer, D.N. Montan, R.A. Nyholm, N.L. Rector, D.G. Wilder and J.L. Yow, Jr., "Spent Fuel Test-Climax: Technical measurements, interim report, fiscal year 1981," Lawrence Livermore National Laboratory, UCRL-53294, (1982).
- Ramspott, L.D., L.B. Ballou, R.C. Carlson, J.E. Duncan, W.C. Patrick, D.G. Wilder, W.G. Brough and M.C. Mayr, "Technical concept for a test of geologic storage of spent reactor fuel in the climax granite, Nevada Test Site," Lawrence Livermore National Laboratory, UCRL-52796 (1979).
- Ramspott, L.D., L.B. Ballou and W.C. Patrick, "Status report on Spent Fuel Test-Climax: A test of geologic storage of High-Level waste in granite," Lawrence Livermore National Laboratory, UCRL-85516, (1981)
- Whitney, J.A. and J.C. Stormer, "The distribution of $\text{NaAlSi}_3\text{O}_8$ between coexisting microcline and plagioclase and its effect on geothermometric calculations," *Am. Min.*, **62**, 687-691.

TABLE I

Average modes^a, by volume percent, for minerals in altered quartz monzonite, exclusive of K-feldspar phenocrysts, corrected for porosity and statistically insignificant variations. Uncertainties are at the 95% confidence interval. After Connolly (1981).

Mineral	Alteration Type				
	Deuteric (19 analyses)	Propylitic (12 analyses)	Argillic (13 analyses)	Phyllic (5 analyses)	Potassic (14 analyses)
Plagioclase	42.85±1.08	39.16±2.38	9.39±1.49	20.45±8.83	11.85±2.46
K-feldspar ^b	17.97±0.82	17.97±0.82	17.97±0.82	17.97±0.82	56.88±3.89
Quartz	27.17±1.23	27.17±1.23	27.17±1.23	27.17±1.23	4.83±2.57
Biotite	5.38±0.53	4.44±0.80	3.26±0.97	--	--
Muscovite ^c	1.48±0.28	3.27±0.74	6.27±3.29	24.59±6.73	12.89±2.55
Chlorite	0.99±0.18	1.28±0.34	0.02±0.04	--	0.04±0.08
Calcite	0.30±0.08	1.34±0.35	8.13±1.94	4.83±1.69	5.20±0.93
Clinzoisite	0.55±0.05	0.55±0.05	--	--	--
Epidote	0.18±0.02	0.18±0.02	--	--	--
Kaolinite	--	0.57±0.85	22.64±5.42	0.52±0.97	--
Smectite	0.07±0.05	0.46±0.37	0.50±0.39	0.22±0.45	--
Titanite	0.44±0.10	0.27±0.10	--	0.05±0.13	--
Rutile	--	0.17±0.12	0.74±0.16	0.54±0.65	0.53±0.16
Magnetite	0.78±0.17	0.31±0.12	--	--	--
Hematite	--	0.13±0.05	0.43±0.17	--	--
Pyrite	0.03±0.03	0.16±0.06	0.15±0.13	1.33±1.04	0.46±0.20

^a Accessories apatite, allanite, hornblende, and zircon do not vary significantly in any of the altered rocks and have average modes of 0.26, 0.04, 0.02, and 0.01 percent, respectively.

^b Includes deuteric K-feldspar that has a mode of 0.10 percent.

^c On the average, 95% of muscovite grains are on plagioclase; the remainder occur on biotite.

TABLE II

MINERAL ASSEMBLAGES FORMED DURING THE
ALTERATION OF PLAGIOCLASE

A.	Pc	(10)
B.	Pc, Mu	(55)
C.	Pc, Mu, Cc	(45)
D.	Pc, Mu, Ep	(8)
E.	Pc, Mu, Ep, Cc	(11)

Number in parentheses indicates the number of regions found with a particular assemblage.

TABLE III

MINERAL ASSEMBLAGES FORMED DURING
THE ALTERATION OF BIOTITE

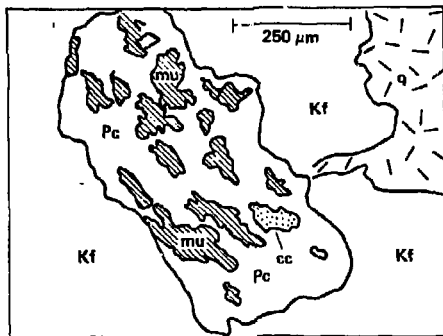
1	Bt	(0)
2	Bt, Chl	(30)
3	Bt, Chl, Mu	(1)
4	Bt, Chl, Ep	(26)
5	Bt, Chl, Tn	(2)
6	Bt, Chl, Mu, Ep	(1)
7	Bt, Chl, Ep, Tn	(5)
8	Bt, Chl, Mu, Tn, Ru	(1)
9	Bt, Chl, Mu, Ep, Tn	(2)
10	Bt, Chl, Ep, Tn, Ru	(1)
11	Bt, Chl, Mu, Ep, Tn, Ru	(2)
12	Chl, Mu, Tn	(6)
13	Chl, Ep, Tn	(4)
14	Chl, Mu, Ep, Tn	(17)
15	Chl, Mu, Tn, Cc	(2)
16	Chl, Mu, Tn, Ru	(3)
17	Chl, Mu, Ru, Cc	(4)
18	Chl, Ep, Tn, Ru	(1)
19	Chl, Mu, Ep, Tn, Cc	(3)
20	Chl, Mu, Ep, Tn, Ru	(4)
21	Chl, Mu, Ep, Ru, Cc	(3)
22	Chl, Mu, Tn, Ru, Cc	(4)
23	Chl, Mu, Ep, Tn, Ru, Cc	(1)
24	Mu, Tn	(4)
25	Mu, Ep, Tn, Cc	(2)

Number in parentheses indicates the number of regions found with a particular assemblage.

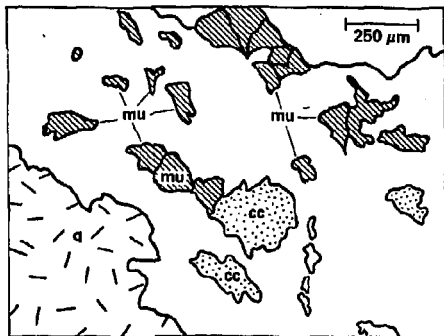
TABLE IV
OBSERVED COMBINATIONS OF BIOTITE AND PLAGIOCLASE
ALTERATION ASSEMBLAGES

A2	(5)	B2	(21)	C4	(1)	D2	(3)	E2	(1)
A4	(5)	B3	(19)	C6	(1)	D4	(1)	E12	(1)
		B4	(1)	C7	(2)	D7	(1)	E14	(7)
		B5	(2)	C8	(1)	D9	(1)	E18	(1)
		B7	(2)	C11	(1)	D14	(2)	E24	(1)
		B9	(2)	C12	(4)				
		B11	(1)	C13	(3)				
		B12	(1)	C14	(6)				
		B13	(1)	C15	(1)				
		B14	(2)	C16	(3)				
		B15	(1)	C17	(4)				
		B20	(1)	C19	(3)				
		B22	(1)	C20	(3)				
				C21	(3)				
				C22	(3)				
				C23	(1)				
				C24	(3)				
				C25	(3)				

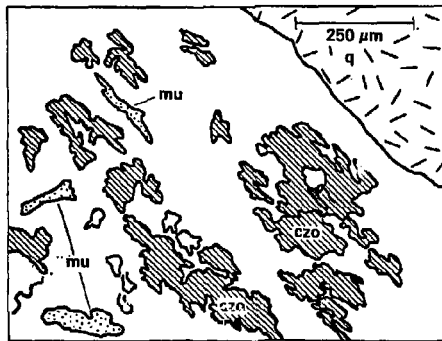
Number in parentheses indicates the number of regions found with a particular assemblage.



A

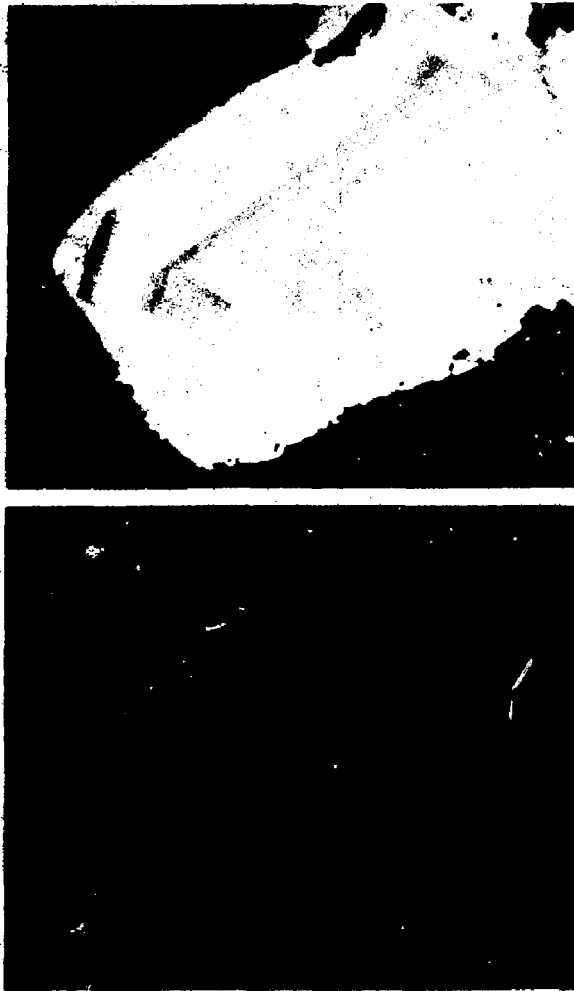


B



C

Fig.1. Tracings of photomicrographs of altered plagioclase. (a) muscovite (mu) and calcite (cc) developed on plagioclase (pc), (b) same features as (a), (c) muscovite and clinzoisite (czo) developed on plagioclase.



(a) Secondary clinozoisite-epidote grain found in plagioclase,
(b) backscattered electron image, (b) Fe_K x-ray image.

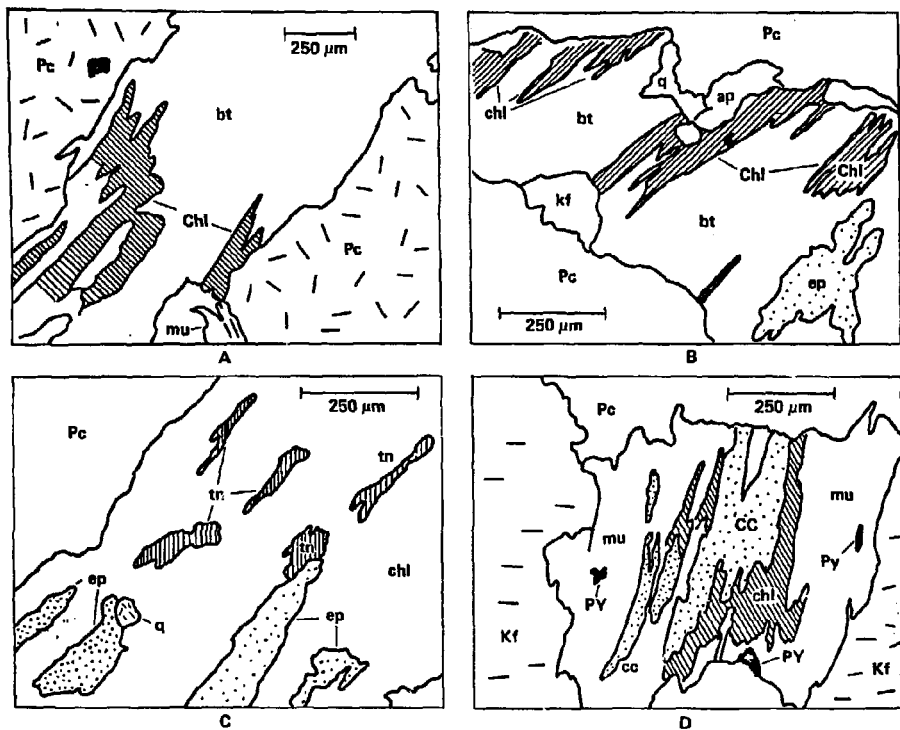
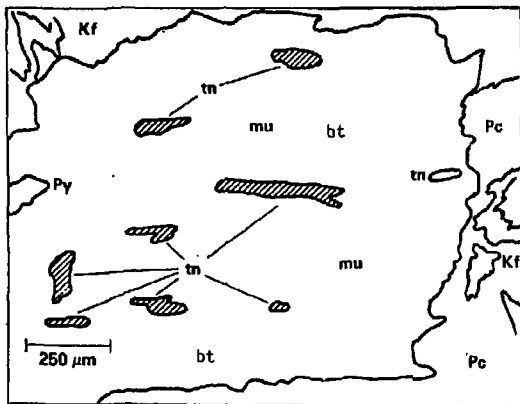
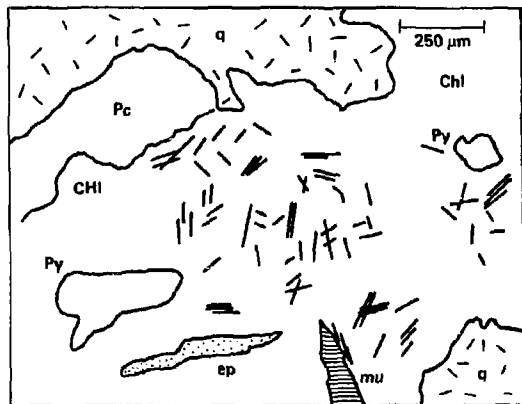


Fig. 3.



E



F

Fig. 3. Tracings of photomicrographs of biotite alteration. (a) Chlorite developed on biotite, (b) chlorite and epidote developed on biotite, (c) epidote, titanite, chlorite and quartz after biotite, (d) chlorite, calcite, muscovite and pyrite after biotite, (e) muscovite, titanite and pyrite after biotite, (f) chlorite, epidote, muscovite, pyrite and rutile (needles) after biotite. Symbols, bt=biotite, chl=chlorite, ep=epidote, tn=titanite, py=pyrite, pc=plagioclase, cc=calcite, mu=muscovite, q=quartz, kf=K-feldspar.

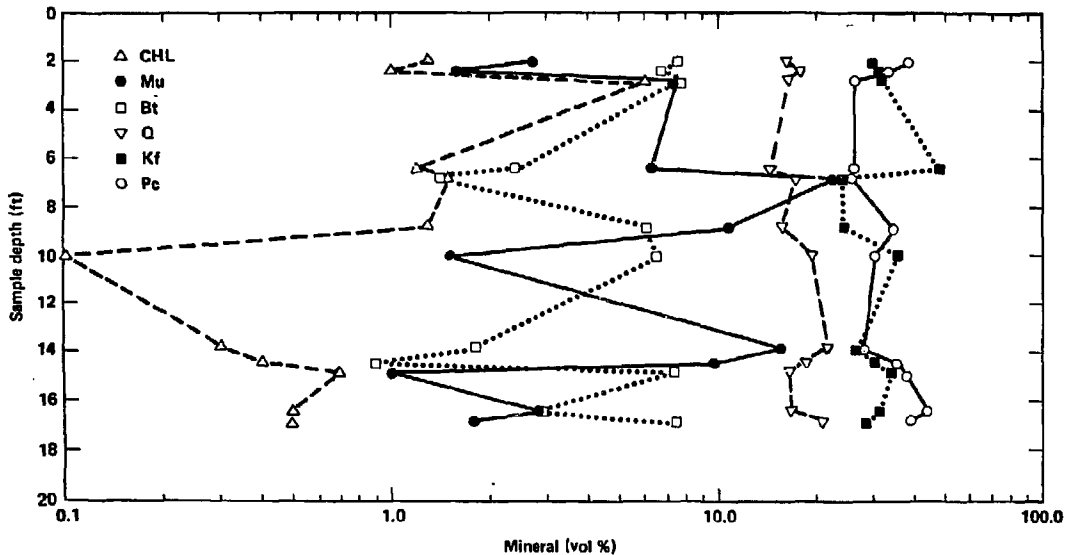


Fig. 4. Modal proportions of major phases in CCH-1 samples plotted versus sample depth.

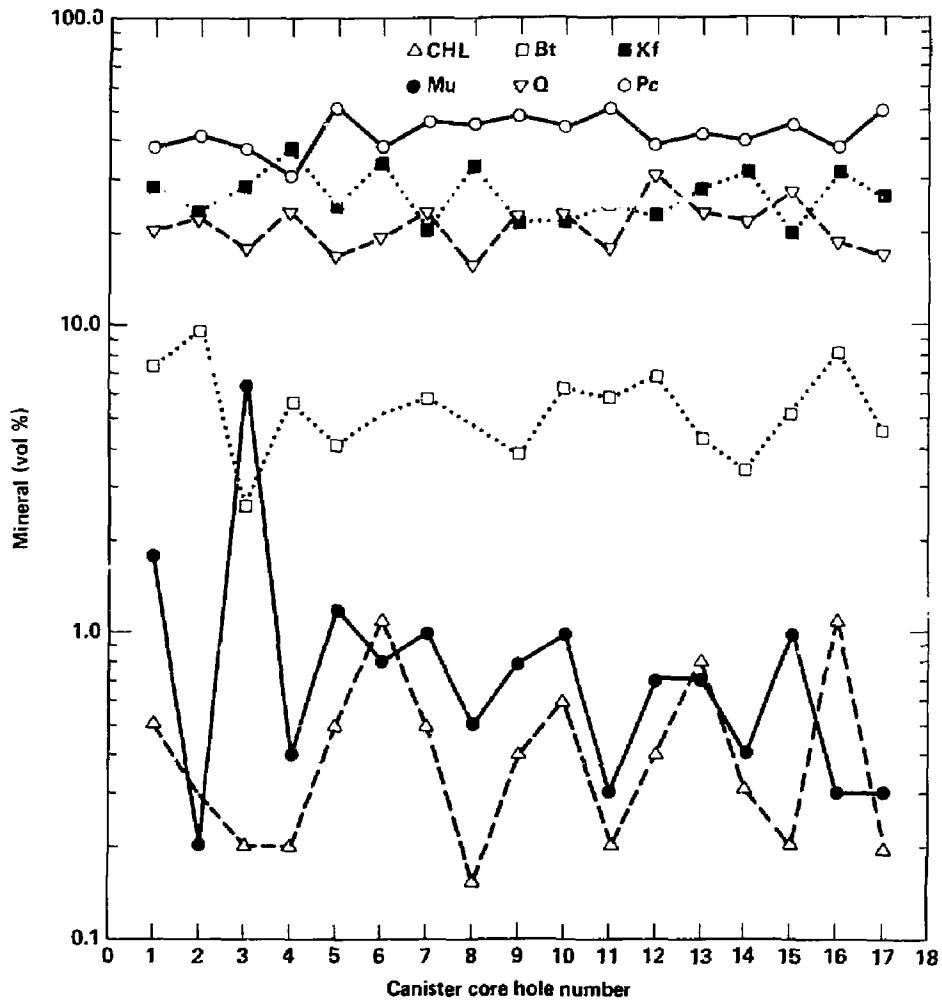


Fig. 5. Modal proportions of major mineral phases from "bulk" samples plotted versus canister core hole position.

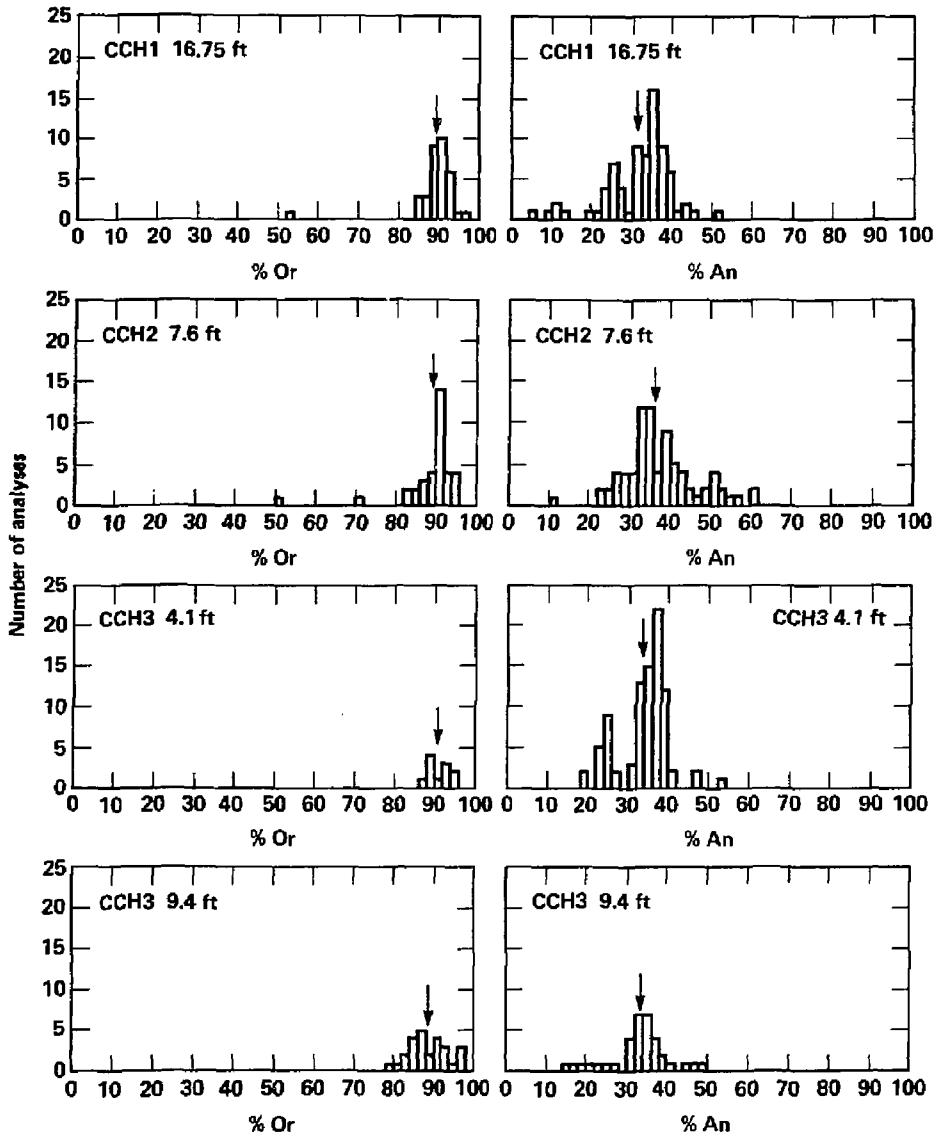


Fig. 6a. Histograms of feldspar analyses, arrows indicate average analysis, depth given in feet.

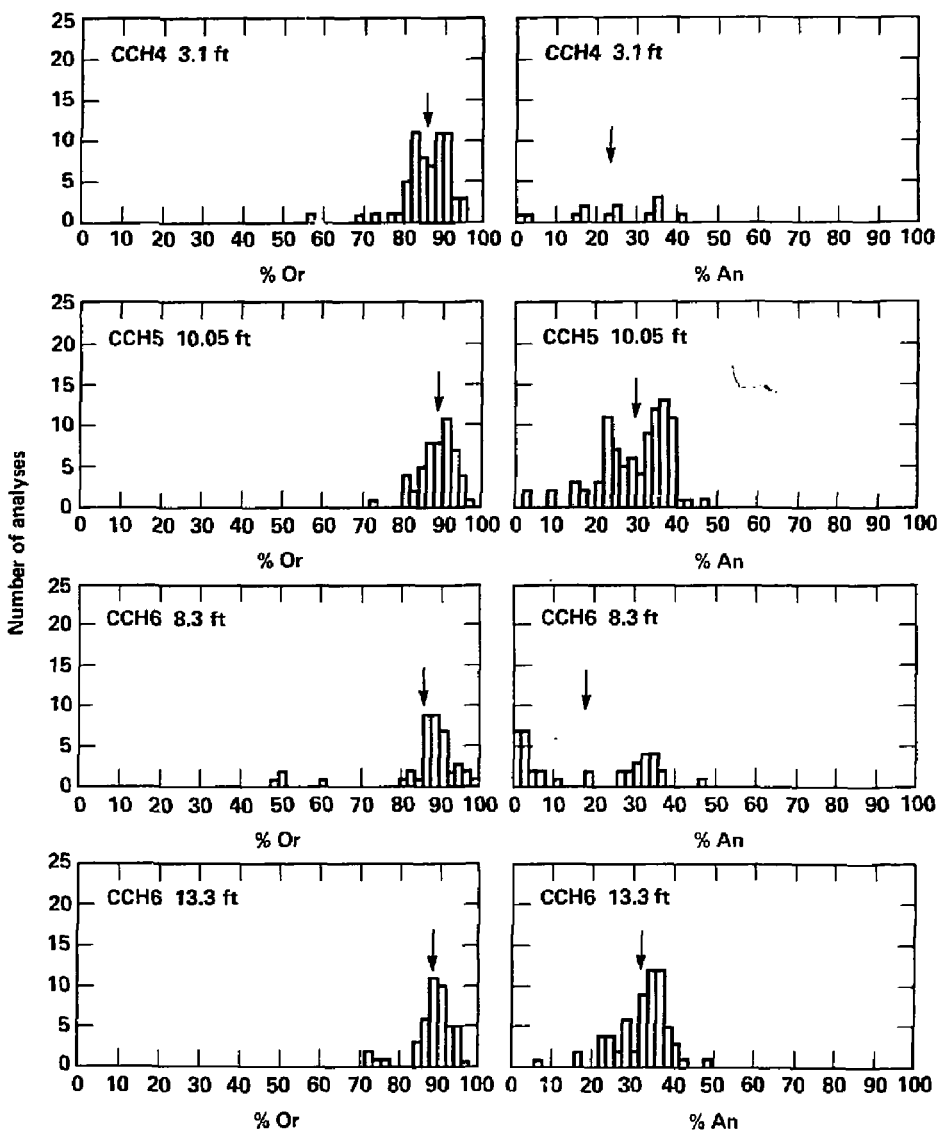


Fig. 6b. Histograms of feldspar analyses, arrows indicate average analysis, depth given in feet.

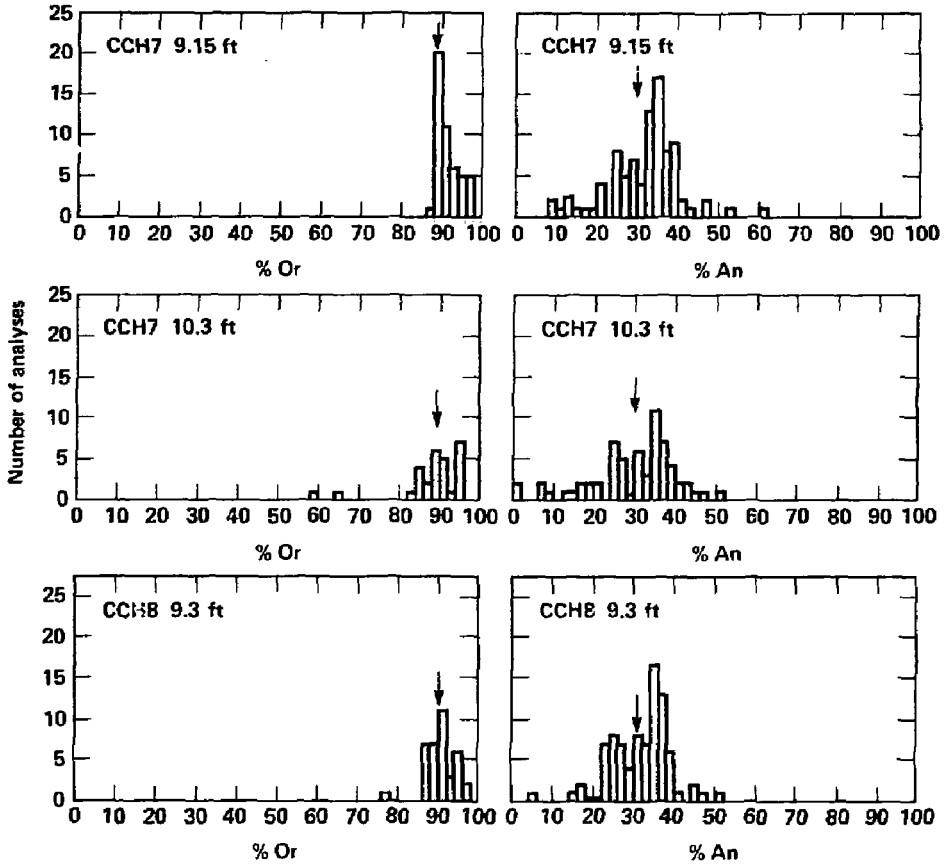


Fig. 6c. Histograms of feldspar analyses, arrows indicate average analysis, depth given in feet.

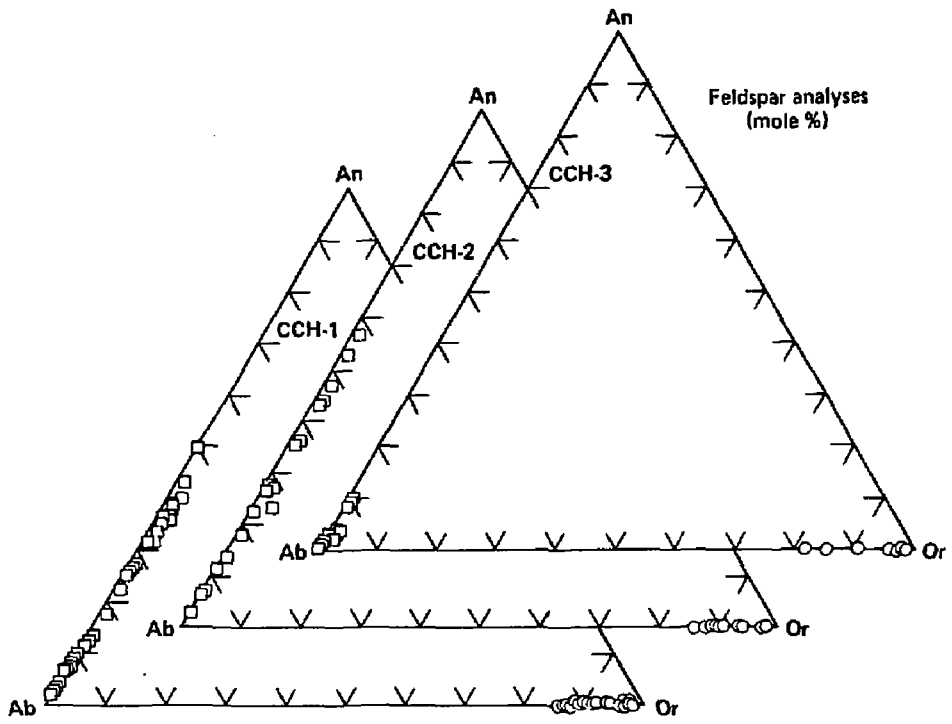


Fig. 7. Plots of feldspar analyses for CCH1, 2, and 3. Analyses obtained in interactive mode.

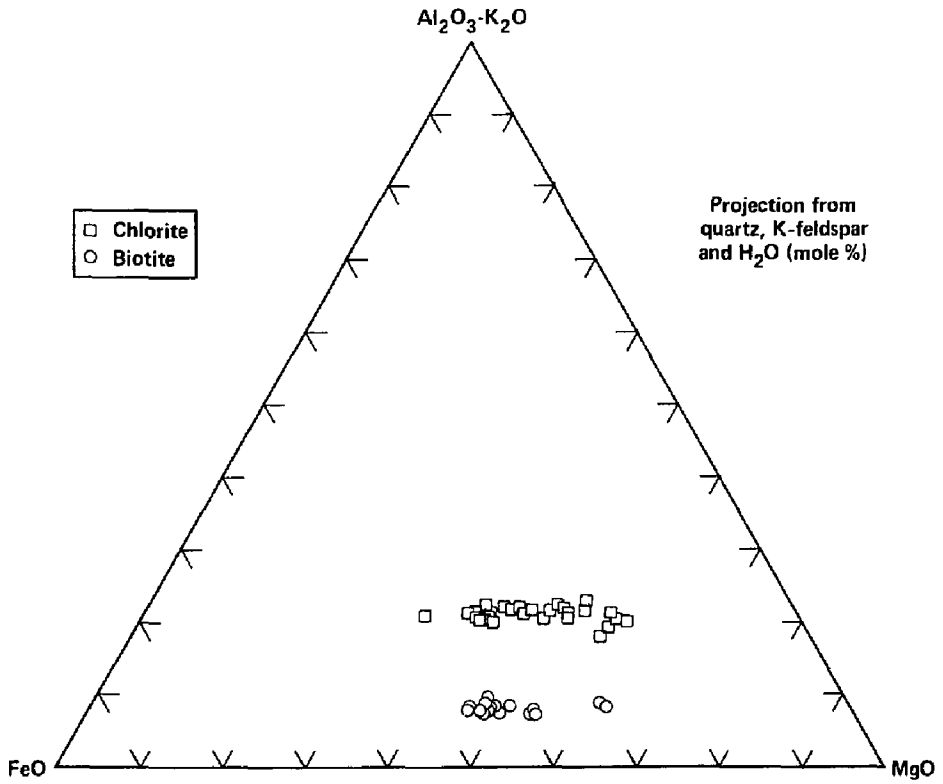


Fig. 8. Projection of biotite and chlorite analyses.

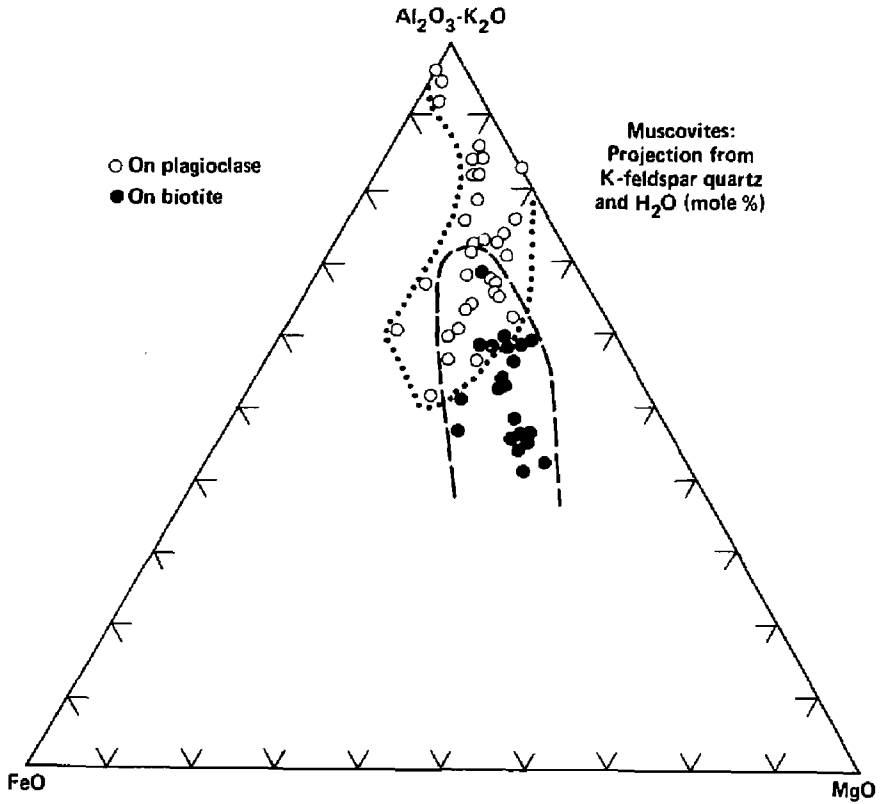


Fig. 9. Projection of muscovite analyses for grains found on biotite and plagioclase.

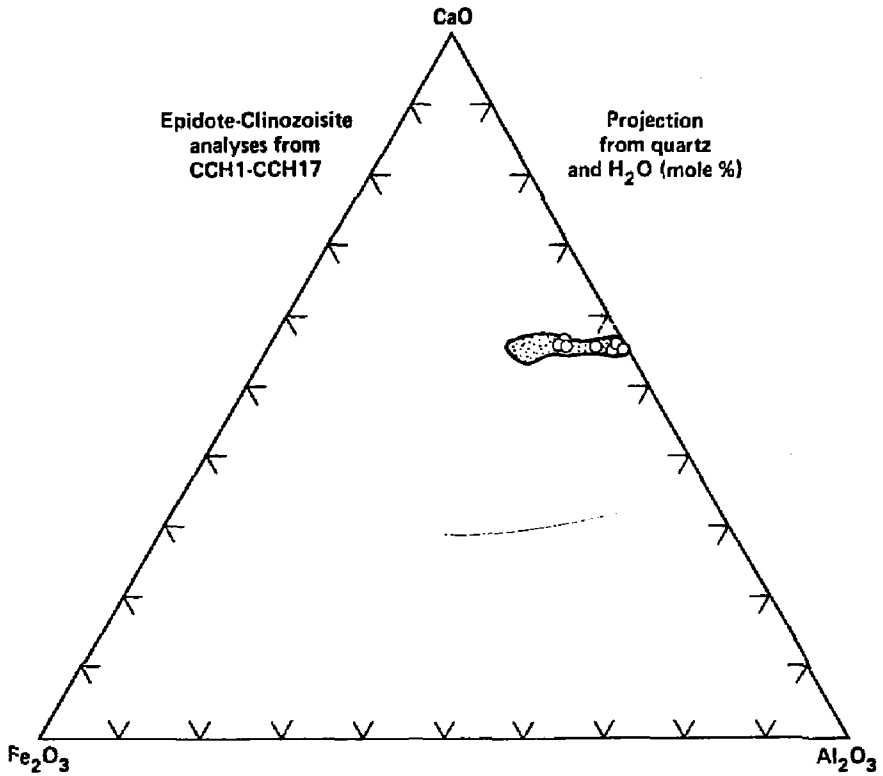


Fig. 10. Projection of epidote and clinozoisite analyses. The stippled field contains all the analyses. The open circles are from a single clinozoisite grain included as a secondary phase in plagioclase (see text and Fig. 2)

APPENDIX A
Secondary Mineral Assemblages

CCH1

DEPTH	Pc					Kf			Bt								
	Pc	Kf	Mu	Ep	Cc	Kf	Mu	Cc	Bt	Chl	Mu	Ep	Tn	Ru	Cc		Py
2.17	W	+				+			+	+							A4
	S	+	+	+	+	+	+			+	+	+	+			+	E14
2.45		+	+		0	+			+	+							B2
2.78	W	+	+			+			+	+							B2
	S	+	+	0		+				+	0	+	+				D14
6.4	W	+	+			+			+	+							B2
	S	+	+			+				+	+	+	+			+	B14
6.75		+	+		+	+				+	+	+	+	+		+	B20
8.75	W	+	+		+					+	+	+	+				C14
	S	+	+	+					+	+		+	+	+			D10
13.8	W	+	+			+			+	+	+						B4
	S	+	+			+	+	+	+	+	+						B4
14.42		+	+		+	+	0	0	0	+	+		+	+		+	C8
14.8		+	+			+			+	+	+	+	+			+/-	B9
16.37		+	+	0	0	+				+		+	+	+		+	E18
16.75		+	+		0	+			+	+	+	+				+	C6

+ indicates phase is present and common

0 indicates phase is present, but only in minor amounts

CCH2

DEPTH	Pc					Kf			Bt							
	Pc	Kf	Mu	Ep	Cc	Kf	Mu	Cc	Bt	Chl	Mu	Ep	Tn	Ru	Cc	
3.35 W S	+		+	0	+	+			+	+		+	0	0		B11 E24
4.10	+		+		0	+			+	+		+	+			C7
6.82																
7.27 W S	+		+			+			+	+		+	+			B2 B13
7.6	+		0			+			+	0						B2
8.0	+		0						+	+		+				B4

CCH3

DEPTH	Pc					Kf			Bt								
	Pc	Kf	Mu	Ep	Cc	Kf	Mu	Cc	Bt	Ch1	Mu	Ep	In	Ru	Cc		Py
3.35	W S	+	+		+	+			+	+		0	+				B7 C20
		+	+		+	+				+	+	+	+	0			
3.7		+	+			+			+	+		0					B4
8.9	W S	+	+		+	+			+	+		0	+			+	B2 C14
		+	+		+	+				+	+	+	+				
9.15		+	+			+			+	+		+					B4
9.4		+	0			+			+	0							B2
10.04	W S	+	+					+	+								D2 E14
		+	+	+					+	+	+	+					
14.45		+	0						+	+							B2 C17
		+	+		+					+	+			+	+	+	
15.0																	

CCH4

DEPTH	Pc					Kf			Bt								
	Pc	Kf	Mu	Ep	Cc	Kf	Mu	Cc	Bt	Ch1	Mu	Ep	Tn	Ru	Cc		Py
2.55	+		+			+			+	+	0	+	+				B9
3.1	+		0			+			+	+							B2
3.83	W S	+	0			+			+	0							B2 E12
9.15	+		+		+	+	+			0	+		+	+	+	+	C22
9.8	+		+		+	+	0		+	+		+	+			+	C7
13.55	+		+		+				+	+		0					C4
14.45	+		+		+	+	0	0		+	+		+				C12

CCH5

DEPTH	Pc					Kf			Bt								
	Pc	Kf	Mu	Ep	Cc	Kf	Mu	Cc	Bt	Chl	Mu	Ep	Tn	Ru	Cc		Py
3.4	+		+		+	+	0				+	+	+		+	+	C25
8.1	+		+			+			+	+		+					B4
9.35	W	+	0			+			+	+							B2
	S	+	+		+	+	0			+	0	+	+			+	C14
10.05		+	0						+	+		0					B4
10.15		+	+		+	+	+			+	+	+	+	+		+	C20
10.2		+	+		0	+	+			+		+	+				C13

CCH6

DEPTH	Pc					Kf			Bt								
	Pc	Kf	Mu	Ep	Cc	Kf	Mu	Cc	Bt	Chl	Mu	Ep	Tn	Ru	Cc		Py
7.75	+		+		+					+	+	+	+	+	+	+	E23
8.30	W	+	0						+	+	+		+	+			B3
	S	+	+		+				+	+	+	0	+	+		+	C11
8.80																	
13.3		+	0						+	+		+				+	B4
13.95		+	+	+	+					+	+	+	+				E14

CCH7

DEPTH	Pc					Kf			Bt								
	Pc	Kf	Mu	Ep	Cc	Kf	Mu	Cc	Bt	Chl	Mu	Ep	Tn	Ru	Cc		Py
9.15																	
9.57	+		+		+					+	+	+	+		+	+	E20
10.3	+		0							+	+		0				B4
10.65	+		0							+	+		0				B4
10.9	W S	+	0							+	+	+					B4 C14
		+	+		+						+	+	+	+			

CCHB

DEPTH	Pc					Kf			Bt								
	Pc	Kf	Mu	Ep	Cc	Kf	Mu	Cc	Bt	Chl	Mu	Ep	Tn	Ru	Cc		Py
9.3	+	+							+	+						+	B2
9.8	+		0						+	+		0				+	B4
10.15	+		+		+	+				+	+	+	+	+		+	* C19
10.55	+		+		0	+				+	+	+	+			+	C14

CCH9

DEPTH	Pc					Kf			Bt								
	Pc	Kf	MU	Ep	Cc	Kf	MU	Cc	Bt	Ch1	Mu	Ep	Tn	Ru	Cc		Py
1.95	W	+	0			+			+	+						+	B2
	S	+	+	+		+	0			+	+	+			+	+	C16
3.25	W	+	0			+			+	+		+					B4
	S	+	+	+		+				+	+		+				C12
3.6		+	0						+	+		0				+	B4
8.2	W	+	+						+	+							B2
	S	+	+	+						+	+		+	+		+	C15
8.7		+	0						+	0							B2
9.4		+	0			+			+	+						+	B2
9.52		+	+	0					+	+		+	+				D7
14.47		+	+		+	+				+	+		+	+	+	+	C16
14.75		+	+						+	+							B2
14.97	+		0						+	+		0					B4
	+	+	+	+						+	+		+	+	+	+	C22
15.60																	

CCH10

DEPTH	Pc					Kf			Bt								
	Pc	Kf	Mu	Ep	Cc	Kf	MU	Cc	Bt	Chl	Mu	Ep	Tn	Ru	Cc		Py
9.15	+		0						+	+		0				+	B4
9.75	+		0			+			+	+		0	+			+	B7
14.84	+		+		+					+	+			+	+	+	C17
15.24 W	+		0						+	+							B2
S	+		+		+					+	+		+			+	C12
15.38	+		+		+	+	+				+		+			+	C24

CCH11

DEPTH	Pc					Kf			Bt							
	Pc	Kf	Mu	Ep	Cc	Kf	Mu	Cc	Bt	Chl	Mu	Ep	Tn	Ru	Cc	Py
9.5	+		0						+	+						B2
9.9																
10.02																

1
2
3

CCH12

DEPTH	Pc					KF			Bt									
	Pc	KF	Mu	Ep	Cc	KF	Mu	Cc	Bt	Chl	Mu	Ep	Tn	Ru	Cc		Py	
9.1	+		+		+	+					+	+	0	+		+	+	C21
9.35	+		0			+					+	+		+			+	B12
9.70	+		+		+	+					0	+		+	0	+		C22
10.18																		

CCH13

DEPTH	Pc					Kf			Bt								
	Pc	Kf	Mu	Ep	Cc	Kf	Mu	Cc	Bt	Chl	Mu	Ep	Tn	Ru	Cc		Py
8.68 W S	+		+						+	+		+					B2 B22
8.93	+		+	+	+					0	+	+	+			+	E14
9.35	+		+		+	+				+	+	0		+	0		C21
9.6	+		0			+			+	+		0					B4

CCH14

DEPTH	Pc					Kf			Bt								
	Pc	Kf	Mu	Ep	Cc	Kf	Mu	Cc	Bt	Chl	Mu	Ep	Jh	Ru	Cc		Py
8.31	+		0			+			+	+		+					B4
8.82	+					+			+	+		+					A4
9.32	W	+	0						+	+		+					B4
	S	+	+		+	+				+	+	+	+		+		C14
9.64	W	+	0						+	+							B2
	S	+	+							+	+	+	+				B14
10.0	+		+	+	+	+			+	+							E2
13.72	+		+	+							+	+	+	+			D14

CCH15

DEPTH	Pc					Kf				Bt							
	Pc	Kf	MU	Ep	Cc	Kf	MU	Cc	Bt	Chi	MU	Ep	Tn	Ru	Cc	Py	
2.35	+		+		+	+	+				+	+	+		+	+	C19
2.75																	
3.05	+		+			+			+	+		+					B4
9.2	+		+		+	+				+	+		+	+		+	C16
9.38	W	+			+	+			+	+			+				A2
	S	+	+		+	+				+	+		+			+	C12
10.0	+		+	+		+			+	+		+					D4
12.47	+								+	+		+					A4
13.27																	

CCH16

DEPTH	Pc					Kf			Bt								
	Pc	Kf	Mu	Ep	Cc	Kf	Mu	Cc	Bt	Chl	Mu	Ep	Tn	Ru	Cc		Py
3.15	+		+		+	+					+		+			+	C24
3.75	+		+		+	+	+				+	0	+		+		C25
9.05	+					+			+	+							A2
9.3	+		+		+					+	+			+	+	+	C17
9.42	+		+		+	+				+	+			+	+		C17

CCH17

DEPTH	Pc					Kf			Bt								
	Pc	Kf	Mu	Ep	Cc	Kf	Mu	Cc	Bt	Ch1	Mu	Ep	Tn	Ru	Cc	Py	
7.45	+								+	+		+					A4
8.05	+		+			+	+		0	+		+	+				B5
8.2	+		+		+	+	+				+		+				C24
8.25	+		+		+	+	+				+		+			+	C24
8.38	+		+							+	+		+		+	+	B15
8.8	+		0						+	+			+				B5
9.1	+		+		+					+	+		+				C12

APPENDIX B1

MODAL ANALYSES (VOL %) OF CCH1 SAMPLES
SAMPLE DEPTH (FT.)

	2.17	2.45	2.78	6.40	6.75	8.75	10.02	13.8	14.42	14.8	16.47	16.75	AVG. 1-8
Plagioclase	36.9	34.1	26.0	26.1	25.3	34.5	29.9	28.1	35.4	37.1	42.3	38.2	32.8±5.6
K-feldspar	30.0	30.8	32.0	44.0	24.4	24.4	35.8	28.2	30.3	34.6	31.3	28.5	31.2±5.3
Quartz	15.1	17.8	16.1	14.5	17.1	15.5	19.1	21.2	18.4	16.2	16.5	20.2	17.3±2.1
Biotite	7.5	6.7	7.6	2.4	1.4	6.0	6.5	1.8	0.9	7.3	2.8	7.4	4.9±2.7
Muscovite	2.7	1.6	7.6	6.3	22.3	10.7	1.5	15.3	9.7	1.0	2.9	1.8	7.0±6.6
Chlorite	1.3	1.0	6.0	1.2	1.5	1.3	0.1	0.3	0.4	0.7	0.5	0.5	1.2±1.5
Calcite	0.7	0.5	0.7	0.3	4.5	3.1	0.1	4.3	2.8	1.1	2.1	1.7	1.8±1.5
Clinozoisite	0.6	--	0.2	--	--	0.8	0.0	--	--	--	--	--	--
Epidote	2.8	0.3	2.1	0.6	0.6	1.4	0.8	0.4	0.3	0.7	0.1	0.3	0.9±0.8
Kspinite	--	--	--	.02	.02	--	--	--	.04	.11	--	--	--
Titanite	0.9	0.2	1.5	1.1	0.7	0.6	0.2	0.2	0.6	0.3	0.0	0.4	0.5±0.4
Rutile	--	--	--	--	0.2	--	--	--	0.0	--	--	--	--
Magnetite	--	0.1	--	--	0.1	0.1	--	--	.04	.11	--	--	--
Hematite	--	--	--	--	--	--	--	--	--	--	--	--	--
Pyrite	1.3	1.3	--	1.1	0.5	0.6	3.6	0.4	1.0	0.2	1.4	0.9	1.0±0.9

APPENDIX B2

MODAL ANALYSES (VOL %) OF "BULK" SAMPLES

Hole	1	2	3	4	5	6	7	8	9	10	11	12	13	14	15	16	17
Depth (ft)	16.75	7.80	10.05	3.10	10.05	8.80	10.65	9.80	8.70	9.75	9.50	10.18	9.60	10.60	10.00	9.05	8.80
Plagioclase	38.2	40.9	37.5	30.5	51.8	37.9	45.8	45.0	47.5	43.3	49.9	36.9	41.3	39.2	44.8	36.7	49.8
K-feldspar	28.5	22.7	27.8	37.5	23.9	33.4	20.3	32.3	21.0	23.8	24.1	21.5	27.2	31.5	19.6	30.6	25.4
Quartz	20.2	22.2	17.9	23.2	16.3	18.9	22.9	15.7	21.6	22.6	17.1	29.0	23.0	21.3	27.0	18.0	16.5
Biotite	7.4	9.4	2.6	5.6	4.0	5.1	5.8	4.8	3.7	6.2	5.7	6.6	4.3	7.4	5.2	8.0	5.4
Muscovite	1.8	0.2	6.1	0.4	1.2	0.8	1.0	0.5	0.8	1.0	0.3	0.6	0.7	0.4	1.0	0.3	0.3
Chlorite	0.5	0.3	0.2	0.2	0.5	1.1	0.5	0.1	0.4	0.6	0.2	0.4	0.8	0.3	0.2	1.1	0.2
Calcite	1.7	0.7	2.4	0.6	0.6	0.4	0.4	0.3	0.4	0.5	0.6	0.6	0.6	0.6	0.3	1.0	0.1
Clinozoisite	0.0	0.0	2.1	0.1	0.2	0.2	0.0	0.0	0.2	0.0	0.0	0.4	0.2	0.2	0.0	0.1	0.0
Epidote	0.3	0.2	0.2	0.3	0.2	0.4	0.5	0.1	1.1	0.8	0.2	0.7	0.2	0.2	0.4	0.4	0.2
Kaolinite	0.0	0.0	0.0	0.0	0.0	0.0	0.0	0.0	0.0	0.0	0.0	0.0	0.0	0.0	0.0	0.0	0.0
Titanite	0.4	1.4	0.8	0.4	0.6	0.4	1.2	0.3	0.2	0.5	0.8	1.0	0.5	1.0	0.3	1.8	0.6
Rutile	0.0	0.2	0.0	0.1	0.0	0.1	0.0	0.0	0.9	0.0	0.1	0.0	0.0	0.0	0.0	0.0	0.0
Magnetite	0.0	0.0	0.0	0.0	0.0	0.0	0.0	0.0	0.0	0.0	0.0	0.0	0.0	0.0	0.0	0.0	0.0
Hematite	0.0	0.0	0.0	0.0	0.0	0.0	0.0	0.0	0.0	0.0	0.0	0.0	0.0	0.0	0.0	0.0	0.0
Pyrite	0.9	1.9	2.3	1.2	1.8	1.4	1.7	1.0	2.6	0.8	0.0	2.1	1.3	1.9	1.3	1.8	1.5

APPENDIX C

Microprobe Analyses of mineral phases
from the canister control hole cores

PLAGIOCLASE ANALYSES

Hole #	1	1	1	1	1	1	1	1	1	1	1	1	1	1	1	1	1	1	1
Depth	2.17	2.17	2.17	2.17	2.17	2.17	2.17	2.17	2.45	2.45	2.45	2.45	2.45	2.78	2.78	2.78	6.40	6.40	6.40
SiO ₂	59.28	61.15	58.68	63.88	59.51	58.05	61.23	58.54	57.38	61.45	62.64	58.72	56.46	66.03	68.26	67.18	61.42	67.45	65.28
TiO ₂	.00	.00	.02	.00	.00	.00	.03	.02	.00	.00	.01	.00	.10	.00	.00	.00	.00	.00	.00
Al ₂ O ₃	25.43	24.51	26.21	23.187	26.55	26.41	24.66	26.62	28.35	24.83	25.07	27.20	28.60	20.11	20.36	22.18	25.16	21.53	22.18
FeO	.12	.14	.11	.00	.00	.00	.02	.11	.12	.00	.15	.00	.00	.02	.00	.00	.21	.02	.05
MgO	.00	.00	.00	.00	.00	.00	.00	.00	.00	.00	.00	.00	.00	.00	.00	.00	.00	.00	.00
MnO	.00	.00	.00	.02	.00	.00	.04	.04	.00	.04	.00	.00	.00	.00	.00	.00	.00	.00	.00
CaO	6.44	5.03	7.30	2.91	7.16	7.97	5.35	7.36	8.96	5.37	5.17	8.04	9.87	.34	.45	1.98	5.62	1.34	2.48
Na ₂ O	7.65	8.30	6.86	9.91	7.75	6.90	8.18	7.01	6.38	8.47	8.48	6.45	5.60	10.90	11.36	10.95	8.07	10.69	10.21
K ₂ O	.20	.26	.33	.06	.26	.33	.26	.24	.19	.26	.26	.40	.11	.05	.04	.04	.25	.06	.08
P ₂ O ₅	.00	.00	.00	.02	.02	.00	.00	.00	.04	.11	.00	.00	.00	.00	.00	.00	.00	.00	.00
F	.00	.00	.00	.00	.00	.00	.00	.00	.00	.00	.00	.00	.00	.00	.00	.00	.00	.00	.00
TOTAL	99.19	99.39	99.52	99.97	101.24	99.65	99.73	99.81	101.44	100.67	101.63	101.20	100.74	97.50	100.50	102.33	100.80	101.09	100.31

PLAGIOCLASE ANALYSES

Hole #	1	1	1	1	1	1	1	1	1	1	2	2	2	2	2	2	2	2	2
Depth	6.40	6.75	6.75	6.75	6.75	6.75	13.8	14.42	16.47	16.47	6.87	6.87	6.87	7.27	7.27	7.27	7.27	7.27	7.27
SiO ₂	65.74	59.22	59.55	59.32	66.01	67.31	67.89	69.43	61.00	60.50	68.15	63.64	60.76	67.47	66.90	63.82	53.59	56.07	54.25
TiO ₂	.28	.01	.04	.00	.00	.00	.00	.00	.00	.00	.03	.00	.00	.03	.00	.05	.02	.00	.42
Al ₂ O ₃	22.49	26.84	26.42	26.54	21.57	20.87	20.63	20.94	25.59	26.91	20.75	24.33	25.67	22.26	21.21	23.56	30.73	28.77	29.14
FeO	.04	.16	.12	.30	.03	.02	.00	.00	.12	.11	.12	.08	.12	.02	.02	.00	.20	.14	.18
MgO	.00	.00	.00	.00	.00	.00	.00	.00	.00	.00	.00	.01	.02	.00	.00	.00	.19	.00	.09
MnO	.00	.05	.01	.00	.00	.01	.02	.00	.04	.01	.02	.00	.04	.00	.01	.02	.00	.00	.00
CaO	2.69	7.27	7.27	6.96	1.69	.81	.40	1.13	6.64	6.87	.61	4.59	5.48	1.41	1.28	3.95	11.50	9.86	10.78
Na ₂ O	10.13	7.00	7.30	7.49	10.33	10.72	11.66	11.67	7.76	7.53	11.12	8.90	8.38	10.70	10.72	9.55	4.82	5.98	5.20
K ₂ O	.06	.26	.20	.28	.11	.09	.16	.07	.30	.16	.00	.14	.18	.08	.03	.14	.23	.23	.25
P ₂ O ₅	.00	.00	.00	.02	.02	.00	.00	.00	.00	.00	.11	.00	.00	.00	.00	.00	.00	.00	.00
F	.00	.00	.00	.00	.00	.00	.00	.00	.00	.00	.00	.00	.00	.00	.00	.00	.00	.00	.00
TOTAL	101.44	100.81	100.91	100.89	99.72	99.84	100.78	102.25	101.43	102.10	100.88	101.68	100.65	101.97	100.18	101.08	101.28	101.06	100.26

PLAGIOCLASE ANALYSES

Hole #	2	2	2	2	2	2	2	2	2	3	3	3	3	3	3	3	3	3	3	
Depth	7.27	8.00	8.00	8.00	8.00	8.00	8.00	8.00	8.00	3.83	3.83	3.83	3.83	3.83	3.83	3.83	3.83	8.90	8.90	8.90
SiO ₂	59.09	66.00	61.69	60.68	58.82	57.26	57.86	65.50	61.96	66.62	65.99	68.59	68.14	68.76	68.40	67.51	68.71	67.44	68.25	
TiO ₂	.06	.00	.28	.00	.00	.14	.04	.00	.08	.13	.00	.14	.00	.15	.00	.23	.00	.00	.00	
Al ₂ O ₃	26.36	22.02	25.08	24.68	26.78	7.69	28.00	22.64	25.70	22.31	22.32	20.92	20.72	20.98	21.27	21.04	20.88	20.90	20.62	
FeO	.21	.00	.21	.17	.15	.19	.75	.03	.03	.19	.10	.00	.05	.03	.02	.00	.00	.08	.00	
MgO	.00	.00	.02	.00	.00	.00	.00	.00	.00	.00	.00	.00	.00	.00	.00	.00	.00	.00	.00	
MnO	.02	.00	.00	.04	.00	.02	.03	.90	.00	.00	.04	.00	.00	.00	.00	.00	.00	.00	.00	
CaO	7.37	2.30	5.59	5.54	7.29	8.63	8.59	2.78	4.85	1.82	1.65	.56	.59	.73	.69	.83	.49	.73	.34	
Na ₂ O	7.26	10.17	8.22	8.10	7.20	6.00	6.01	9.86	8.47	10.64	10.65	11.69	11.36	11.41	11.18	11.34	11.39	11.05	11.63	
K ₂ O	.29	.10	.37	.31	.19	.19	.19	.14	.57	.14	.07	.03	.04	.03	.22	.16	.08	.11	.09	
P ₂ O ₅	.00	.00	.00	.00	.00	.00	.00	.00	.00	.00	.00	.00	.00	.00	.00	.00	.00	.00	.00	
F	.00	.00	.00	.00	.00	.00	.00	.00	.00	.00	.00	.00	.00	.00	.00	.00	.00	.00	.00	
TOTAL	100.65	100.60	101.47	99.48	100.46	100.13	101.44	100.98	102.16	101.85	100.77	101.92	100.89	102.08	101.77	101.18	101.55	100.29	100.94	

PLAGIOCLASE ANALYSES

Hole #	3	3	3	3	4	4	6	6
Depth	8.90	14.45	14.45	14.45	9.15	9.15	7.75	7.75
SiO ₂	66.87	68.98	67.80	68.60	67.74	67.55	66.15	68.32
TiO ₂	.00	.00	.00	.00	.13	.90	.00	.00
Al ₂ O ₃	21.74	20.41	20.83	21.06	20.94	20.83	23.40	21.46
FeO	.04	.00	.13	.00	.00	.00	.00	.07
MgO	.00	.00	.00	.00	.00	.00	.00	.02
MnO	.00	.00	.00	.00	.00	.00	.00	.00
CaO	1.98	.10	.84	.56	.74	.55	2.53	.43
Na ₂ O	10.67	11.86	11.27	11.59	11.51	11.19	10.29	10.83
K ₂ O	.08	.09	.08	.11	.08	.04	.08	.63
P ₂ O ₅	.00	.00	.00	.00	.00	.00	.00	.00
F	.00	.00	.00	.00	.00	.00	.00	.00
TOTAL	101.34	101.44	100.94	101.92	101.14	100.25	102.45	101.76

K-FELDSPAR ANALYSES

Hole #	1	1	1	1	1	1	1	1	1	1	1	1	1	1	1	1	1	1	1
Depth	2.17	2.17	2.17	2.45	2.45	2.45	2.45	2.78	2.78	6.40	6.40	6.40	6.40	6.40	6.40	6.75	6.75	6.75	6.75
SiO ₂	64.02	64.00	64.41	65.25	65.34	65.11	66.47	65.28	615.10	65.02	64.80	65.26	64.70	65.44	64.67	65.53	64.61	64.52	64.54
TiO ₂	.03	.39	.00	.00	.00	.01	.00	.00	.00	.01	.00	.00	.00	.02	.06	.00	.05	.00	.00
Al ₂ O ₃	19.16	19.29	19.13	19.71	19.22	19.37	19.07	19.75	19.02	19.50	19.41	19.73	19.13	18.91	19.23	18.62	20.00	19.44	18.77
FeO	.06	.08	.00	.06	.05	.03	.11	.05	.04	.08	.05	.00	.08	.09	.04	.07	.03	.05	.06
MgO	.00	.00	.00	.00	.00	.00	.00	.00	.00	.00	.00	.00	.00	.00	.00	.00	.00	.00	.00
MnO	.00	.00	.00	.01	.00	.02	.00	.04	.04	.00	.00	.07	.03	.04	.00	.00	.00	.01	.00
CaO	.00	.03	.00	.11	.00	.02	.00	.08	.04	.08	.06	.02	.00	.03	.03	.01	.02	.00	.02
Na ₂ O	1.28	.99	1.10	1.58	1.38	1.18	1.22	1.50	1.25	1.41	1.25	.98	.99	1.11	.36	1.11	.29	.61	.35
K ₂ O	14.95	15.58	15.22	14.25	14.92	15.32	15.14	14.92	15.44	14.38	14.59	15.27	15.15	15.52	15.96	15.30	16.32	16.13	16.25
P ₂ O ₅	.00	.00	.13	.11	.00	.00	.00	.00	.09	.04	.00	.05	.00	.00	.00	.00	.00	.00	.00
F	.00	.00	.00	.00	.00	.00	.00	.00	.00	.00	.00	.00	.00	.00	.00	.00	.00	.00	.00
TOTAL	99.55	100.34	99.99	101.09	100.90	101.06	102.01	101.67	100.98	100.60	100.16	101.36	100.08	101.16	100.34	100.64	101.32	100.78	99.99

K-FELDSPAR ANALYSES

Hole #	1	1	1	1	1	1	1	1	1	1	1	1	1	1	1	1	1	2	2
Depth	6.40	6.75	6.75	6.75	6.75	6.75	13.80	14.42	16.47	16.47	16.47	16.47	16.47	16.47	16.47	16.47	16.47	6.87	6.87
SiO ₂	64.90	64.61	64.52	64.54	64.90	63.56	63.19	63.99	66.15	64.62	65.95	64.57	66.00	65.43	65.43	65.64	65.30	65.37	65.54
TiO ₂	.06	.05	.00	.00	.06	.03	.00	.04	.00	.13	.12	.00	.03	.00	.00	.03	.00	.07	.09
Al ₂ O ₃	19.33	20.00	19.44	18.77	19.33	19.10	18.67	19.26	19.02	19.27	19.72	19.78	19.68	19.81	19.62	19.49	19.25	19.04	19.07
FeO	.02	.03	.05	.06	.02	.00	.00	.02	.00	.00	.00	.15	.04	.06	.00	.02	.00	.15	.07
MgO	.03	.00	.00	.00	.03	.04	.00	.00	.00	.00	.00	.00	.00	.00	.00	.00	.00	.00	.02
MnO	.00	.00	.01	.00	.00	.00	.03	.05	.00	.00	.00	.05	.00	.00	.00	.01	.00	.00	.03
CaO	.07	.02	.00	.02	.07	.00	.00	.00	.02	.00	.02	.02	.00	.02	.01	.00	.00	.02	.00
Na ₂ O	1.13	.29	.61	.35	1.13	.40	.39	.26	.27	.35	.64	1.09	1.26	1.06	1.12	1.10	1.05	.21	1.06
K ₂ O	14.95	16.32	16.13	16.25	14.95	16.20	16.26	16.46	16.35	16.54	15.85	15.33	14.80	15.32	15.30	15.25	15.78	16.36	15.54
P ₂ O ₅	.00	.00	.00	.00	.00	.06	.00	.00	.00	.00	.00	.00	.00	.00	.00	.00	.00	.00	.00
F	.00	.00	.00	.00	.00	.00	.00	.00	.00	.00	.00	.00	.00	.00	.00	.00	.00	.00	.00
TOTAL	100.49	101.32	100.78	99.99	100.49	99.50	98.55	100.26	101.80	101.04	102.27	100.98	100.87	101.71	101.56	101.56	101.38	101.21	101.42

K-FELDSPAR ANALYSES

Hole #	2	2	2	2	2	2	2	2	2	2	3	3	3	3	3	3	3	3		
Depth	6.87	6.87	6.87	6.87	6.87	6.87	7.27	8.00	8.00	8.00	8.00	3.83	3.83	3.83	3.83	10.04	10.04	10.04	10.04	14.45
SiO ₂	65.54	65.22	64.69	63.51	64.54	65.87	64.42	65.11	65.43	65.72	63.76	64.88	65.03	62.17	64.65	65.92	64.71	64.86	.00	.00
TiO ₂	.09	.16	.16	.29	.00	.04	.00	.00	.02	.02	.00	.89	.00	.00	.57	.00	.15	.42	.00	.00
Al ₂ O ₃	19.07	18.59	19.69	19.32	18.77	19.48	18.53	19.00	18.98	18.87	18.70	19.14	19.21	18.70	19.44	19.26	19.38	18.98	.00	.00
FeO	.07	.12	.07	.11	.07	.04	.05	.14	.05	.00	.08	.00	.07	.07	.00	.00	.00	.00	.00	.00
MgO	.02	.02	.02	.00	.01	.00	.00	.00	.00	.00	.02	.02	.00	.00	.00	.00	.00	.00	.00	.00
MnO	.03	.03	.03	.00	.01	.00	.00	.03	.00	.04	.00	.00	.03	.00	.00	.00	.00	.00	.00	.00
CaO	.00	.00	.02	.09	.00	.00	.00	.03	.00	.00	.00	.00	.00	.00	.00	.05	.00	.00	.00	.00
Na ₂ O	1.06	1.01	1.31	1.50	.70	1.06	.63	1.20	1.13	.51	.18	.20	.28	.11	.25	.25	1.08	1.64	.00	.00
K ₂ O	15.54	15.39	14.55	14.50	15.90	15.53	15.98	14.95	14.83	15.92	16.28	16.36	16.34	16.80	16.29	16.07	14.86	14.28	.00	.00
P ₂ O ₅	.00	.00	.00	.00	.00	.00	.00	.00	.00	.00	.00	.00	.00	.00	.00	.00	.00	.00	.00	.00
F	.00	.00	.00	.00	.00	.00	.00	.00	.00	.00	.00	.00	.00	.00	.00	.00	.00	.00	.00	.00
TOTAL	101.42	100.54	100.55	99.33	100.50	102.01	99.60	100.46	100.44	100.90	99.02	101.49	100.98	97.94	101.13	101.56	100.18	100.17	.00	.00

K-FELDSPAR ANALYSES

Hole #	6	6
Depth	7.75	7.75
SiO ₂	65.01	65.07
TiO ₂	.00	.00
Al ₂ O ₃	19.55	19.19
FeO	.14	.00
MgO	.04	.04
MnO	.00	.00
CaO	.03	.02
Na ₂ O	.24	.22
K ₂ O	16.29	16.64
P ₂ O ₅	.00	.00
F	.00	.00
TOTAL	101.30	101.83

BIOTITE ANALYSES

Hole #	1	1	1	1	1	1	1	1	1	1	1	1	1	2	2	2	2
Depth	2.17	2.45	2.45	2.45	2.78	2.78	6.40	6.40	6.75	6.75	6.75	16.44	16.47	7.27	7.27	8.00	8.00
SiO ₂	35.98	36.29	36.91	34.61	37.99	37.45	37.82	37.59	37.24	37.72	36.47	36.93	37.98	36.56	35.89	36.54	37.76
TiO ₂	3.19	2.75	3.0	3.43	.35	2.08	3.38	3.59	2.72	2.54	3.13	3.47	3.65	2.62	3.67	3.50	3.04
Al ₂ O ₃	15.28	15.28	14.66	15.30	15.44	15.44	16.16	15.92	16.66	15.58	15.40	15.80	16.15	15.32	15.13	15.04	15.32
FeO	18.20	18.78	18.79	18.92	16.49	16.62	12.84	13.21	18.99	19.08	19.38	17.71	18.03	18.80	19.51	18.75	18.92
MgO	11.37	11.46	11.29	11.48	12.96	12.61	15.26	15.03	11.55	12.37	11.03	12.16	12.30	12.00	11.00	11.28	11.59
MnO	.59	.64	.56	.55	.75	.80	.94	.99	.60	.67	.67	.62	.68	.66	.58	.58	.57
CaO	.02	.02	.05	.02	.00	.12	.03	.03	.02	.02	.00	.02	.00	.02	.05	.02	.00
Na ₂ O	.03	.15	.10	.09	.11	.10	.03	.04	.07	.04	.03	.10	.12	.12	.12	.08	.10
K ₂ O	9.68	9.23	9.23	9.65	10.18	9.56	9.81	9.61	9.66	9.91	9.62	9.81	10.00	9.66	9.55	9.35	9.49
P ₂ O ₅	.06	.04	.00	.00	.16	.00	.05	.00	.02	.00	.06	.11	.11	.00	.00	.06	.00
F	.44	.92	.36	.26	.74	.71	.68	.41	.51	.50	.56	.65	.33	.40	.43	.46	.62
TOTAL	94.84	95.56	95.08	94.52	95.16	95.49	97.10	96.41	98.05	98.43	96.33	97.37	98.93	96.17	95.93	95.66	97.41

EPIDOTE ANALYSES

Hole #	1	1	1	1	1	1	2	2	2	2	2	2	3	3	3	3	
Depth	2.17	2.17	2.17	2.78	2.78	2.78	6.87	6.87	6.87	6.87	7.27	8.00	8.00	8.90	8.90	10.04	10.04
SiO ₂	35.83	37.77	37.16	38.32	38.67	38.32	38.02	37.88	37.92	38.58	37.58	37.64	37.46	37.88	39.20	38.46	37.37
TiO ₂	.00	.52	.20	.00	.00	.00	.35	.54	.11	1.52	.19	1.17	.28	.00	.00	.15	.87
Al ₂ O ₃	24.34	24.92	24.89	24.08	25.64	24.74	21.90	23.02	22.38	24.90	21.66	21.95	22.20	28.09	27.89	24.23	23.03
FeO	11.84	11.12	10.43	11.57	10.71	12.12	14.20	13.37	14.58	9.85	14.57	13.64	13.64	8.23	7.59	12.58	13.37
MgO	.00	.01	.02	.05	.25	.05	.00	.13	.01	.14	.03	.04	.00	.00	.00	.41	.02
MnO	.00	.17	.22	.45	.30	.96	.16	.24	.10	.17	.12	.22	0.56	.05	.00	.29	.22
CaO	23.56	23.26	23.65	23.23	23.72	22.94	22.98	22.83	22.84	23.39	23.21	22.92	21.85	22.73	23.32	23.05	22.19
Na ₂ O	.00	.00	.00	.00	.00	.00	.00	.00	.02	.00	.00	.00	.00	.00	.02	.00	.00
K ₂ O	.03	.00	.03	.00	.07	.00	.00	.01	.00	.00	.00	.02	.02	.01	.04	.00	.03
P ₂ O ₅	.00	.00	.00	.00	.00	.00	.00	.02	.14	.00	.00	.00	.00	.15	.05	.00	.06
F	.00	.00	.00	.00	.00	.00	.07	.15	.00	.13	.08	.18	.00	.00	.00	.00	.00
TOTAL	95.60	97.77	96.57	97.70	97.66	99.13	97.70	98.20	98.12	98.68	97.42	97.08	96.01	97.16	98.51	99.17	97.15

EPIDOTE ANALYSES

Hole #	4	4	4	4	4	4	4	4	4	4	6	6	6
Depth	3.83	3.83	3.83	3.83	3.83	3.83	3.83	9.15	9.15	9.15	7.75	7.75	7.75
SiO ₂	38.21	38.36	38.54	36.85	38.30	37.80	38.05	38.36	37.73	37.49	38.81	38.43	37.64
TiO ₂	.03	.10	.00	.20	.00	.24	.00	.41	.01	.29	.00	.00	.00
Al ₂ O ₃	25.88	27.97	25.25	28.64	28.88	25.68	26.48	25.19	24.03	23.01	25.53	25.17	25.08
FeO	10.48	8.17	9.35	6.77	6.50	9.33	9.46	10.54	12.55	13.76	11.71	11.16	11.60
MgO	.11	.04	.04	.04	.05	.04	.13	.00	.00	.00	.08	.03	.19
MnO	1.00	.32	.65	.10	.14	.19	.09	.20	.15	.54	.12	.41	.27
CaO	22.46	23.33	22.92	23.40	23.97	22.86	23.31	22.77	21.13	21.49	22.67	23.23	22.20
Na ₂ O	.00	.00	.00	.00	.00	.62	.00	.00	.00	.00	.00	.00	.00
K ₂ O	.00	.00	.00	.02	.00	.20	.01	.07	.03	.03	.02	.03	.02
P ₂ O ₅	.00	.08	.00	.00	.05	.08	.05	.11	.14	.04	.00	.03	.00
F	.00	.00	.00	.00	.00	.00	.12	.00	.00	.00	.00	.00	.00
TOTAL	98.19	98.38	98.73	98.01	97.90	97.03	97.69	97.66	95.80	96.88	98.93	98.48	97.00

MUSCOVITE ANALYSES

Hole #	1	1	1	1	1	1	1	1	1	1	1	1	1
Depth	2.17	2.17	2.17	2.17	2.78	6.40	6.40	6.40	6.75	6.75	6.75	6.75	6.75
SiO ₂	46.15	47.23	46.05	45.59	47.09	47.00	46.82	48.26	46.20	50.14	49.70	49.43	50.73
TiO ₂	.44	.40	.33	.48	.00	.12	.00	.48	.02	.00	.06	.00	.06
Al ₂ O ₃	29.17	31.13	27.41	28.49	30.32	36.96	39.23	30.08	37.79	30.98	32.27	32.22	31.06
FeO	4.86	3.78	4.42	4.56	3.98	1.11	.77	3.42	.65	2.34	2.22	1.86	2.87
MgO	2.67	3.31	5.06	5.00	2.92	.31	.17	3.85	.00	2.39	1.91	2.00	2.02
MnO	.00	.04	.03	.04	.03	.35	.07	.00	.06	.04	.17	.03	.02
CaO	.00	.00	.00	.00	.06	.03	.00	.00	.00	.00	.00	.00	.05
Na ₂ O	.17	.12	.13	.12	.15	.20	.24	.16	.07	.11	.11	.09	.08
K ₂ O	10.89	10.60	10.70	10.64	10.84	9.82	10.34	10.40	10.51	10.94	10.87	10.77	10.98
F ₂ O ₅	.00	.00	.00	.00	.00	.00	.00	.12	.09	.00	.00	.00	.00
F	.04	.40	.00	.18	.36	.00	.00	.20	.24	.20	.07	.00	.00
TOTAL	94.39	97.01	94.13	95.10	95.75	95.88	97.63	96.98	95.62	97.13	97.37	96.42	97.87

MUSCOVITE ANALYSES

Hole #	1	1	1	1	1	1	1	1	1	1	1	1	1	1	1	1	1	1	
Depth	13.80	13.80	13.80	13.80	13.80	13.80	13.80	13.80	14.42	14.42	14.42	14.42	14.42	14.42	14.42	14.42	14.42	16.47	16.47
SiO ₂	50.68	50.40	47.08	47.03	47.83	48.13	47.94	46.33	48.45	50.03	48.92	47.11	48.24	49.03	48.24	47.09	49.75	47.58	46.47
TiO ₂	.11	.00	.87	.49	.03	.09	.41	.49	.00	.06	.53	.70	.95	.03	.63	.44	.07	.71	.35
Al ₂ O ₃	29.61	30.79	30.12	28.40	30.09	29.96	30.59	27.92	30.36	32.71	33.47	30.00	29.75	31.86	31.08	27.23	32.31	30.41	29.19
FeO	2.98	2.88	2.99	3.34	2.04	3.22	3.38	4.02	1.40	.85	.00	2.94	3.11	2.48	2.78	4.24	1.47	3.84	4.60
MgO	2.23	2.05	3.05	3.80	2.52	3.23	3.78	4.99	2.28	2.23	1.87	3.23	3.31	2.32	3.74	5.74	2.18	2.86	4.78
MnO	.03	.10	.02	.07	.09	.04	.08	.06	.00	.00	.00	.00	.00	.60	.04	.00	.00	.01	.06
CaO	.05	.00	.03	.20	.05	.02	.02	.02	.05	.00	.04	.07	.02	.04	.61	.00	.03	.00	.00
Na ₂ O	.07	.07	.18	.20	1.11	.21	.22	.16	.06	.10	.10	1.13	1.15	.18	.25	.15	.16	.14	.14
K ₂ O	10.88	11.19	11.13	10.83	10.74	10.95	11.33	10.97	10.88	10.97	10.66	10.69	10.94	10.75	11.12	11.03	10.60	11.07	10.91
F ₂ O ₅	.00	.06	.00	.02	.02	.06	.00	.02	.05	.00	.00	.00	.00	.00	.07	.00	.00	.00	.05
F	.00	.12	.00	.12	.10	.12	.15	.17	.14	.20	.00	.16	.00	.12	.43	.23	.14	.07	.11
TOTAL	96.64	97.66	95.47	94.32	93.60	96.02	97.91	95.13	95.72	97.14	95.59	95.07	96.58	96.82	98.38	96.21	96.71	96.70	96.67

MUSCOVITE ANALYSES

Hole #	2	2	2	2	2	2	2	2	3	3	3	3	3	3
Depth	5.87	7.27	7.27	7.27	8.00	8.00	8.00	8.00	8.90	8.90	8.90	10.04	10.04	10.04
SiO ₂	45.69	46.36	49.62	46.78	47.73	46.81	46.62	49.69	49.95	48.39	48.23	48.15	47.52	
TiO ₂	1.67	.68	.06	.33	.42	.23	.43	.00	.00	.00	.29	.76	.05	
Al ₂ O ₃	30.28	27.93	29.39	27.81	30.64	28.52	29.32	32.37	32.62	33.43	34.97	35.76	34.38	
FeO	4.35	6.44	4.07	6.23	6.01	6.42	6.30	1.66	1.23	1.07	.71	.84	1.29	
MgO	2.48	3.76	3.19	4.28	1.70	3.11	1.85	1.97	1.84	1.70	1.19	1.32	1.31	
MnO	.12	.03	.02	.05	.05	.05	.13	.00	.00	.12	.00	.00	.00	
CaO	.05	.02	.03	.00	.03	.00	.13	.10	.07	.08	.02	.00	.01	
Na ₂ O	.06	.14	.16	.17	.17	.18	.00	.15	.15	.17	.18	.22	.20	
K ₂ O	11.12	10.66	10.64	10.33	10.46	10.36	9.97	10.09	10.56	10.41	10.63	11.00	10.52	
P ₂ O ₅	.04	.09	.05	.00	.00	.00	.11	.05	.05	.00	.06	.02	.10	
F	.29	.15	.31	.14	.00	.00	.11	.00	.00	.00	.00	.00	.08	
TOTAL	97.14	92.64	97.50	96.13				96.09	96.48	95.36	96.28	98.06	95.46	

MUSCOVITE ANALYSES

Hole #	3	3	3	3	3	3	3	3	4	4	4	4	4
Depth	14.45	14.45	14.45	14.45	14.45	14.45	14.45	14.45	9.15	9.15	9.15	9.15	9.15
SiO ₂	48.96	49.39	46.12	46.45	46.91	47.20	47.37	47.64	47.56	47.43	48.02	47.98	47.52
TiO ₂	.00	.00	.46	.00	.00	.55	.00	.00	.00	1.09	.75	.07	.61
Al ₂ O ₃	28.67	30.80	28.27	28.02	29.45	34.82	32.79	34.15	30.19	29.38	32.48	30.81	30.03
FeO	2.17	2.23	4.32	4.69	3.94	.86	1.49	1.23	2.88	3.31	1.59	2.41	2.20
MgO	2.94	2.42	4.61	5.17	3.92	1.29	1.51	1.30	2.73	3.32	1.60	2.59	2.59
MnO	.00	.00	.05	.05	.00	.00	.60	.00	.00	.00	.00	.02	.00
CaO	.09	.12	.03	.08	.05	.07	.09	.07	.04	.04	.04	.02	.00
Na ₂ O	.02	.03	.03	.05	.07	.09	.09	.07	.10	.12	.14	.17	.09
K ₂ O	10.67	11.04	10.81	11.10	11.07	10.85	10.79	10.94	11.33	11.10	10.58	11.36	11.10
P ₂ O ₅	.00	.05	.09	.60	.00	.12	.05	.16	.04	.15	.00	.04	.00
F	.31	.26	.31	.29	.13	.00	.17	.00	.13	.11	.07	.00	.00
TOTAL	94.04	96.33	95.06	96.10	96.09	95.30	94.33	95.57	96.09	95.70	95.02	96.01	93.91

NUSCOVITE ANALYSES

Hole #	6	6	6	6	6	6	6	6	6
Depth	7.75	7.75	7.75	7.75	7.75	7.75	7.75	7.75	7.75
SiO ₂	48.21	50.30	46.78	46.42	47.61	47.24	50.35	49.73	49.04
TiO ₂	.00	.00	.00	.00	.00	.00	.00	.00	.00
Al ₂ O ₃	29.24	28.56	29.90	29.45	31.17	30.38	31.47	32.64	30.82
FeO	3.62	4.87	3.79	4.29	4.99	4.64	3.58	3.66	2.30
MgO	3.68	3.39	2.97	4.10	2.15	2.69	3.12	2.25	2.84
MnO	.00	.00	.00	.04	.02	.00	.00	.00	.00
CaO	.03	.04	.00	.02	.02	.03	.04	.05	.01
Na ₂ O	.10	.07	.15	.11	.18	.15	.13	.16	.13
K ₂ O	11.08	11.07	10.86	10.45	10.84	11.34	10.88	10.58	10.91
F ₂ O ₅	.00	.05	.00	.00	.00	.00	.00	.03	.00
F ⁻	.23	.24	.10	.05	.08	.07	.00	.19	.23
TOTAL	96.19	98.59	94.56	94.93	97.07	96.55	98.56	97.29	96.29

CLINOZOISITE ANALYSES

Hole #	1	2	2	2	2	2	3	3	3	3	3	3	3	3	3	3	
Depth	2.17	3.83	3.83	3.83	7.27	7.27	8.90	8.90	8.90	8.90	8.90	10.04	10.04	10.04	10.04	10.04	
SiO ₂	38.60	39.41	39.62	39.28	38.99	38.56	39.69	39.70	39.43	39.73	39.87	38.52	39.08	38.81	38.52	38.70	38.70
TiO ₂	.00	.19	.00	.00	.07	.08	.00	.00	.00	.00	.00	.20	.64	.05	.47	.22	.59
Al ₂ O ₃	34.31	34.02	33.69	31.34	30.79	31.41	33.11	32.55	31.32	33.72	34.39	29.24	29.57	28.86	28.90	26.34	28.10
FeO	.65	.89	1.02	3.90	4.44	3.65	2.02	1.59	4.00	1.29	.36	6.23	6.31	6.75	7.45	9.79	8.08
MgO	.08	.00	.01	.08	.04	.09	.00	.00	.02	.12	.00	.03	.03	.04	.03	.03	.08
MnO	.12	.00	.00	.99	.53	.80	.70	.43	.00	.00	.00	.55	.44	.39	.59	.10	1.51
CaO	25.17	24.60	24.76	22.96	23.68	24.03	23.10	23.38	23.33	24.01	24.08	23.03	23.14	23.60	23.08	23.57	21.74
Na ₂ O	.00	.02	.00	.00	.00	.00	.02	.03	.00	.04	.00	.00	.00	.00	.00	.00	.00
K ₂ O	.01	.04	.02	.01	.00	.00	.01	.00	.02	.03	.00	.00	.00	.00	.00	.00	.00
P ₂ O ₅	.02	.00	.00	.23	.10	.06	.12	.00	.08	.00	.00	.02	.24	.02	.13	.00	.31
F	.00	.00	.00	.00	.00	.00	.00	.00	.00	.00	.00	.00	.00	.00	.00	.00	.00
TOTAL	98.96	99.16	99.12	98.79	98.65	98.68	98.77	97.68	98.20	98.93	98.80	97.82	99.44	98.52	99.15	98.76	98.90

CHLORITE ANALYSES

Hole #	1	1	1	1	1	1	1	1	1	1	1	1	1	1	1	1	1	2	2	2
Depth	2.45	2.45	2.78	2.78	2.78	2.78	2.78	6.40	6.75	6.75	6.75	6.75	14.42	16.47	16.47	16.47	16.47	6.87	6.87	6.87
SiO ₂	27.20	25.65	27.40	28.17	28.28	29.03	28.96	28.56	26.55	25.78	26.50	25.86	29.48	28.36	26.81	26.99	26.61	28.43	27.18	
TiO ₂	.44	.00	.00	.00	.00	.00	.00	.00	.00	.00	.20	.09	1.35	.22	.08	.18	.13	3.32	.00	
Al ₂ O ₃	19.34	20.45	20.10	19.60	21.15	19.09	17.83	19.37	19.87	20.95	20.51	19.57	20.27	19.26	22.15	20.72	19.24	17.84	19.07	
FeO	24.57	24.08	18.69	19.24	17.48	16.36	17.37	14.25	26.19	24.35	25.81	26.80	15.43	21.82	18.47	18.42	24.65	22.26	28.95	
MgO	15.72	15.40	19.95	20.85	20.40	22.32	22.10	22.50	14.76	14.83	14.54	15.15	22.70	16.53	19.59	19.57	15.57	13.74	12.03	
MnO	.93	.95	.83	.79	.87	1.02	.88	.87	.97	1.14	.61	1.44	.20	.66	.48	.44	.87	.72	.50	
CaO	.33	.06	.02	.03	.03	.03	.03	.01	.00	.01	.05	.02	.07	.06	.02	.00	.03	2.76*	.05	
Na ₂ O	.00	.00	.00	.80	.00	.00	.00	.00	.00	.00	.02	.00	.00	.00	.00	.00	.00	.00	.00	
K ₂ O	.03	.02	.00	.12	.17	.00	.00	.07	.00	.00	.00	.04	.01	.94	.00	.00	.03	.61	.00	
P ₂ O ₅	.04	.04	.12	.05	.00	.09	.16	.00	.00	.00	.00	.00	.00	.00	.00	.00	.04	.04	.02	
F	.21	.00	.15	.17	.14	.00	.00	.00	.00	.00	.00	.00	.39	.00	.00	.00	.11	.12	.00	
TOTAL	89.01	86.65	87.27	89.82	88.50	87.93	87.34	85.63	88.33	87.06	88.23	86.97	89.89	87.85	87.69	86.37	87.28	89.85	87.60	

CHLORITE ANALYSES

Hole #	2	2	2	2	2	2	2	2	3	3	4	4	6	6	6	6	6
Depth	6.87	6.87	7.27	7.27	8.00	8.00	8.00	8.00	10.04	10.04	3.83	3.83	7.75	7.75	7.75	7.75	7.75
SiO ₂	25.55	25.79	25.31	26.61	25.99	26.91	27.87	25.74	26.75	27.46	27.06	27.15	27.53	26.88	27.22	27.20	27.45
TiO ₂	.02	.05	.08	.01	.04	.12	.00	.08	1.63	.02	1.54	.03	.00	.00	.00	.00	.00
Al ₂ O ₃	29.59	21.01	21.00	20.53	20.50	20.65	20.27	20.10	20.69	20.43	21.52	21.39	20.00	21.14	19.90	20.38	20.08
FeO	24.35	23.71	21.33	23.66	24.38	25.06	24.41	25.33	22.00	22.89	18.68	20.34	21.13	21.99	25.39	25.60	25.18
MgO	14.83	15.89	16.24	16.16	15.08	15.76	15.31	14.77	16.80	16.25	19.01	18.77	18.72	17.83	15.46	15.36	15.23
MnO	.90	.85	.57	.61	.55	.48	.48	.55	.79	.70	.72	.84	.17	.15	.60	.79	.80
CaO	.02	.05	.00	.06	.03	.04	.05	.00	.04	.02	.02	.00	.03	.05	.04	.04	.04
Na ₂ O	.00	.00	.00	.00	.03	.00	.08	.00	.12	.00	.08	.00	.00	.05	.00	.00	.00
K ₂ O	.00	.01	.04	.00	.02	.00	.02	.01	.19	.05	.05	.02	.03	.02	.00	.00	.00
P ₂ O ₅	.00	.02	.00	.00	.00	.00	.00	.00	.00	.00	.09	.20	.00	.00	.06	.00	.00
F	.00	.00	.00	.21	.00	.00	.00	.00	.00	.10	.04	.13	.00	.00	.00	.00	.00
TOTAL	85.65	87.38	84.57	87.85	86.62	89.02	88.49	86.58	89.02	87.92	88.78	88.86	87.60	88.13	88.92	89.37	88.78